M Kraus et al.

GEMPIC: Geometric ElectroMagnetic Particle-In-Cell Methods

Preprint of Paper to be submitted for publication in
Physics of Plasmas

GEMPIC: Geometric ElectroMagnetic Particle-In-Cell Methods

Michael Kraus[1,2], Katharina Kormann[1,2], Philip J. Morrison[3], Eric Sonnendrücker[1,2]

[1]Max-Planck-Institut für Plasmaphysik
Boltzmannstraße 2, 85748 Garching, Deutschland

[2]Technische Universität München, Zentrum Mathematik
Boltzmannstraße 3, 85748 Garching, Deutschland

[3]Department of Physics and Institute for Fusion Studies
The University of Texas at Austin, Austin, TX, 78712, USA

September 9, 2016

Abstract

We present a novel framework for finite element particle-in-cell methods based on the discretization of the underlying Hamiltonian structure of the Vlasov-Maxwell system. We derive a semi-discrete Poisson bracket, which satisfies the Jacobi identity, and apply Hamiltonian splitting schemes for time integration. Techniques from Finite Element Exterior Calculus and spline differential forms ensure conservation of the divergence of the magnetic field and Gauss' law as well as stability of the field solver. The resulting methods are gauge-invariant, feature exact charge conservation and show excellent long-time energy behavior.

Contents

1 Introduction

We consider structure preserving numerical implementation of the Vlasov-Maxwell system, the system of kinetic equations, describing the dynamics of charged particles in a plasma, coupled to Maxwell's equations, describing electrodynamic phenomena arising from the motion of the particles as well as from externally applied fields. While the design of numerical methods for the Vlasov-Maxwell (and Vlasov-Poisson) system has attracted considerable attention since the early 1960s (see [70] and references therein), the systematic development of structure-preserving or geometric numerical methods started only recently.

The Vlasov-Maxwell system exhibits a rather large set of structural properties, which should be considered in the discretization. Most prominently, the Vlasov-Maxwell system features a variational [48, 80, 20] as well as a Hamiltonian [58, 78, 59, 51] structure. This implies a range of conserved quantities, which by Noether's theorem are related to symmetries of the Lagrangian and the Hamiltonian, respectively. In addition, the degeneracy of the Poisson brackets in the Hamiltonian formulation implies the conservation of several families of so-called Casimir functionals (see e.g. [56] for review).

Maxwell's equations have a rich structure themselves. The various fields and potentials appearing in these equations are most naturally described as differential forms [11, 76, 75, 5] (see also [34, 55, 30]). The spaces of these differential forms build what is called a deRham complex. This implies certain compatibility conditions between the spaces, essentially boiling down to the identities from vector calculus, $\text{curl}\,\text{grad} = 0$ and $\text{div}\,\text{curl} = 0$. It has been realised that it is of utmost importance to preserve this complex structure in the discretization in order to obtain stable numerical methods. This goes hand-in-hand with preserving the constraints on the electromagnetic fields, $\text{div}\,\mathbf{B} = 0$ and Gauss' law $\text{div}\,\mathbf{E} = \rho$, which constitute two more structural properties.

The compatibility problems of discrete Vlasov-Maxwell solvers has been widely discussed in the Particle-In-Cell (PIC) literature [74, 73, 6, 36, 35, 82] for exact charge conservation. An alternative is to modify Maxwell's equations by adding Lagrange multipliers to relax the constraint [62, 10, 50, 47, 63]. For a more geometric perspective on charge conservation based on Whitney forms one can refer to [54]. Even though it has attracted less interest the problem also exists for grid based discretizations of the Vlasov equations and the same recipes apply there as discussed in [28, 69]. Note also that the infinite-dimensional kernel of the curl operator has made it particularly hard to find good discretization for Maxwell's equations, especially for the eigenvalue problem [7, 8, 13, 19, 43].

Geometric Eulerian (grid-based) discretizations have been proposed based on spline differential forms [4] as well as variational integrators [45]. Recently, also various discretizations based on discontinuous Galerkin methods have been proposed [68, 31, 32, 42, 23, 24, 25, 26, 49]. Even though these are usually not based on geometric principles, they tend to show good long-time conservation properties with respect to e.g. momentum and/or energy.

First attempts to obtain geometric integrators for Particle-in-Cell methods have been made by Squire et al. [71], applying a discrete action principle to Low's Lagrangian for the Vlasov-Maxwell system [48] and discretising the electromagnetic fields via discrete exterior calculus (DEC) [44, 33, 72]. This leads to gauge-invariant variational integrators that satisfy exact charge conservation in addition to approximate energy conservation. Evstatiev and Shadwick [37] performed a variational semi-discretization in space, but

used more standard finite difference and finite element discretizations of the fields and an explicit symplectic integrator in time. As a result, their integrators preserve momentum and energy but not charge. In this work there also appears the first integrator based on a semi-discretization of the noncanonical Poisson bracket formulation of the Vlasov-Maxwell system [58, 78, 59, 51], which automatically leads to gauge-invariant integrators solving for the electromagnetic fields instead of the potentials. In a similar fashion, Xiao et al. [79] suggest a Hamiltonian discretization using Whitney form interpolants for the fields. As these preserve the deRham sequence structure of the involved spaces, their algorithm is also charge conserving. However, both of these works lack a proof of the Jacobi identity for the semi-discrete bracket, which is crucial for a Hamiltonian integrator and He et al. [41] introduce a Hamiltonian discretization based on first order Finite Elements, which is a special case of our structure.

In this work, we unify these ideas in a general, flexible and rigorous framework based on Finite Element Exterior Calculus (FEEC) [2, 3, 27, 53]. We provide a semi-discretization of the Vlasov-Maxwell Poisson structure, which preserves the defining properties of the bracket, anti-symmetry and the Jacobi-identity. This semi-discrete bracket is used in conjunction with splitting methods in order to obtain a fully discrete numerical scheme.

We proceed as follows. In Section 2, we provide a short review of the Vlasov-Maxwell system and its Poisson bracket formulation, including a discussion of the Jacobi identity, Casimir invariants and invariants commuting with the specific Vlasov-Maxwell Hamiltonian. In Section 3, we introduce the Finite Element Exterior Calculus framework using the example of Maxwell's equation, we introduce the deRham complex and finite element spaces of differential forms. The actual discretization of the Poisson bracket is performed in Section 4. We prove the discrete Jacobi identity, the conservation of discrete Casimirs, including the discrete Gauss' law. In Section 5, we introduce a splitting for the Vlasov-Maxwell Hamiltonian, which leads to an explicit time-stepping scheme. Various compositions are used in order to obtain higher order methods. Backward error analysis is used in order to study the long-time energy behavior. In Section 6, we apply the method to the Vlasov-Maxwell system in 1d2v using splines for the discretization of the fields. Section 7 concludes the paper with numerical experiments, using nonlinear Landau damping and the Weibel instability to verify the favorable properties of our scheme.

2 The Vlasov-Maxwell System

The non-relativistic Vlasov equation for a particle species s of charge q_s and mass m_s reads

$$\frac{\partial f_s}{\partial t} + \mathbf{v} \cdot \nabla_{\mathbf{x}} f_s + \frac{q_s}{m_s}(\mathbf{E} + \mathbf{v} \times \mathbf{B}) \cdot \nabla_{\mathbf{v}} f = 0, \tag{1}$$

which couples nonlinearly to the Maxwell equations,

$$\frac{\partial \mathbf{E}}{\partial t} - \operatorname{curl} \mathbf{B} = -\mathbf{J}, \tag{2}$$

$$\frac{\partial \mathbf{B}}{\partial t} + \operatorname{curl} \mathbf{E} = 0, \tag{3}$$

$$\operatorname{div} \mathbf{E} = \rho, \tag{4}$$

$$\operatorname{div} \mathbf{B} = 0. \tag{5}$$

4

These equations are to be solved with suitable initial and boundary conditions. Here, f_s is the phase space distribution function of particle species s, $\mathbf{E}$ and $\mathbf{B}$ are the electric and magnetic fields, respectively. The source for the Maxwell equations, the charge density ρ and the current density $\mathbf{J}$, are obtained from the Vlasov equations by

$$\rho = \sum_s q_s \int f_s \mathrm{d}\mathbf{v}, \quad \mathbf{J} = \sum_s q_s \int f_s \mathbf{v} \mathrm{d}\mathbf{v}. \tag{6}$$

Taking the divergence of Ampère's equation (2) and using Gauss' law (4) gives the continuity equation for charge conservation

$$\frac{\partial \rho}{\partial t} + \operatorname{div} \mathbf{J} = 0. \tag{7}$$

Equation (7) serves as a compatibility condition for Maxwell's equations, which are ill-posed when (7) is not satisfied. Moreover it can be shown that if the divergence constraints (4)-(5) are satisfied at the initial time, they remain satisfied for all times by the solution of Ampère's equation (2) and Faraday's law (3), which have a unique solution by themselves provided adequate initial and boundary conditions are imposed. This follows directly from the fact that the divergence of the curl vanishes and Eq. (7). The continuity equation follows from the Vlasov equation by integrating them over velocity space and using the definitions of charge and current densities. However this does not necessarily remain true when the charge and current densities are approximated numerically. The problem for numerical methods is then to find a way to have discrete sources, which satisfy a discrete continuity equation compatible with the discrete divergence and curl operators. Another option is to modify the Maxwell equations, so that they are well posed independently of the sources, by introducing two additional scalar unknowns that can be seen as Lagrange multipliers for the divergence constraints. These should become arbitrarily small when the continuity equation is close to being satisfied.

2.1 Noncanonical Hamiltonian Structure

The Vlasov-Maxwell system possesses a noncanonical Hamiltonian structure. The system of equations (1)-(3) can be obtained from the following Poisson bracket, a biliniear, anti-symmetric bracket that satisfies Leibniz' rule and the Jacobi identity:

$$\begin{aligned}
\{F, G\}[f_s, \mathbf{E}, \mathbf{B}] = &\sum_s \int \frac{f_s}{m_s} \left[\frac{\delta F}{\delta f_s}, \frac{\delta G}{\delta f_s} \right] \mathrm{d}\mathbf{x}\, \mathrm{d}\mathbf{v} \\
&+ \sum_s \frac{q_s}{m_s} \int f_s \left(\frac{\partial}{\partial \mathbf{v}} \frac{\delta F}{\delta f_s} \cdot \frac{\delta G}{\delta \mathbf{E}} - \frac{\partial}{\partial \mathbf{v}} \frac{\delta G}{\delta f_s} \cdot \frac{\delta F}{\delta \mathbf{E}} \right) \mathrm{d}\mathbf{x}\, \mathrm{d}\mathbf{v} \\
&+ \sum_s \frac{q_s}{m_s^2} \int f_s \mathbf{B} \cdot \left(\frac{\partial}{\partial \mathbf{v}} \frac{\delta F}{\delta f_s} \times \frac{\partial}{\partial \mathbf{v}} \frac{\delta G}{\delta f_s} \right) \mathrm{d}\mathbf{x}\, \mathrm{d}\mathbf{v} \\
&+ \int \left(\nabla \times \frac{\delta F}{\delta \mathbf{E}} \cdot \frac{\delta G}{\delta \mathbf{B}} - \nabla \times \frac{\delta G}{\delta \mathbf{E}} \cdot \frac{\delta F}{\delta \mathbf{B}} \right) \mathrm{d}\mathbf{x}.
\end{aligned} \tag{8}$$

This bracket was introduced in [58], with a term corrected in [51] (see also [78, 59]), and its limitation to divergence free magnetic fields first pointed out in [59]. See also [21] and [57], where the latter contains the details of the direct proof of the Jacobi identity

$$\{F, \{G, H\}\} + \{G, \{H, F\}\} + \{H, \{F, G\}\} = 0. \tag{9}$$

5

The time evolution of any functional $F[f_s, \mathbf{E}, \mathbf{B}]$ is given by

$$\frac{\mathrm{d}}{\mathrm{d}t} F[f_s, \mathbf{E}, \mathbf{B}] = \{F, \mathcal{H}\}, \tag{10}$$

with the Hamiltonian $\mathcal{H}$ given as the sum of the kinetic energy of the particles and the electric and magnetic field energies,

$$\mathcal{H} = \sum_s \frac{m_s}{2} \int |\mathbf{v}|^2 f_s(\mathbf{x}, \mathbf{v}) \, \mathrm{d}\mathbf{x} \, \mathrm{d}\mathbf{v} + \frac{1}{2} \int \left(|\mathbf{E}(\mathbf{x})|^2 + |\mathbf{B}(\mathbf{x})|^2 \right) \mathrm{d}\mathbf{x}. \tag{11}$$

In order to obtain the Vlasov equations, we consider the functional

$$\delta_{\mathbf{xv}}[f_s] = \int f_s(\mathbf{x}', \mathbf{v}') \, \delta(\mathbf{x} - \mathbf{x}') \, \delta(\mathbf{v} - \mathbf{v}') \, \mathrm{d}\mathbf{x}' \, \mathrm{d}\mathbf{v}' = f_s(\mathbf{x}, \mathbf{v}), \tag{12}$$

for which the equations of motion (10) are computed as

$$\begin{aligned}
\frac{\partial f_s}{\partial t}(\mathbf{x}, \mathbf{v}) = & \int \delta(\mathbf{x} - \mathbf{x}') \, \delta(\mathbf{v} - \mathbf{v}') \left[\tfrac{1}{2} |\mathbf{v}'|^2, f_s(\mathbf{x}', \mathbf{v}') \right] \mathrm{d}\mathbf{x}' \, \mathrm{d}\mathbf{v}' \\
& - \frac{q_s}{m_s} \int \delta(\mathbf{x} - \mathbf{x}') \, \delta(\mathbf{v} - \mathbf{v}') \left(\frac{\partial f_s}{\partial \mathbf{v}}(\mathbf{x}', \mathbf{v}') \right) \cdot \mathbf{E}(\mathbf{x}') \, \mathrm{d}\mathbf{x}' \, \mathrm{d}\mathbf{v}' \\
& - \frac{q_s}{m_s} \int \delta(\mathbf{x} - \mathbf{x}') \, \delta(\mathbf{v} - \mathbf{v}') \left(\frac{\partial f_s}{\partial \mathbf{v}}(\mathbf{x}', \mathbf{v}') \right) \cdot (\mathbf{B}(\mathbf{x}') \times \mathbf{v}') \, \mathrm{d}\mathbf{x}' \, \mathrm{d}\mathbf{v}' \\
= & -\mathbf{v} \cdot \frac{\partial f_s}{\partial \mathbf{x}}(\mathbf{x}, \mathbf{v}) - \frac{q_s}{m_s} \left(\mathbf{E}(\mathbf{x}) + \mathbf{v} \times \mathbf{B}(\mathbf{x}) \right) \cdot \frac{\partial f_s}{\partial \mathbf{v}}(\mathbf{x}, \mathbf{v}). \tag{13}
\end{aligned}$$

For the electric field, we consider

$$\delta_{\mathbf{x}}[\mathbf{E}] = \int \mathbf{E}(\mathbf{x}') \, \delta(\mathbf{x} - \mathbf{x}') \, \mathrm{d}\mathbf{x}' = \mathbf{E}(\mathbf{x}), \tag{14}$$

so that from (10) we obtain Ampère's equation,

$$\frac{\partial \mathbf{E}}{\partial t} = \int \left(\nabla \times \mathbf{B}(\mathbf{x}') - \sum_s q_s f_s(\mathbf{x}', \mathbf{v}') \, \mathbf{v}' \right) \delta(\mathbf{x} - \mathbf{x}') \, \mathrm{d}\mathbf{x}' \, \mathrm{d}\mathbf{v}' = \nabla \times \mathbf{B}(\mathbf{x}) - \mathbf{J}(\mathbf{x}), \tag{15}$$

where the current density $\mathbf{J}$ is given by

$$\mathbf{J}(\mathbf{x}) = \sum_s q_s \int f_s(\mathbf{x}, \mathbf{v}) \, \mathbf{v} \, \mathrm{d}\mathbf{v}. \tag{16}$$

And for the magnetic field, we consider

$$\delta_{\mathbf{x}}[\mathbf{B}] = \int \mathbf{B}(\mathbf{x}') \, \delta(\mathbf{x} - \mathbf{x}') \, \mathrm{d}\mathbf{x}' = \mathbf{B}(\mathbf{x}), \tag{17}$$

and obtain the Faraday equation,

$$\frac{\partial \mathbf{B}}{\partial t} = - \int \left(\nabla \times \mathbf{E}(\mathbf{x}') \right) \delta(\mathbf{x} - \mathbf{x}') \, \mathrm{d}\mathbf{x} = -\nabla \times \mathbf{E}(\mathbf{x}). \tag{18}$$

Our aim is to preserve this noncanonical Hamiltonian structure and its features at the discrete level. This can be done by taking only a finite number of initial positions for

6

the particles instead of a continuum and by taking the electromagnetic fields in finite-dimensional subspaces of the original function spaces. This is provided by a Finite Element discretization. A good candidate for such a discretization is the Finite Element Particle-In-Cell framework. In order to satisfy the continuity equation as well as the identities from vector calculus and thereby preserve Gauss' law and the divergence of the magnetic field, the Finite Element spaces for the different fields cannot be chosen independently. The right framework is given by Finite Element Exterior Calculus (FEEC).

Before describing this framework in more detail, we shortly want to discuss the Jacobi identity of the bracket (8) as well as some conservation laws of the Vlasov-Maxwell system. In Hamiltonian systems, there are two kinds of conserved quantities, momentum maps and Casimirs.

2.2 Invariants

A family of conserved quantities are Casimir invariants (Casimirs), which originate from the degeneracy of the Poisson bracket. Casimirs are functionals $\mathcal{C}(f, \mathbf{E}, \mathbf{B})$ which Poisson commute with every other functional $\mathcal{G}(f, \mathbf{E}, \mathbf{B})$, i.e., $\{\mathcal{C}, \mathcal{G}\} = 0$.

For the Vlasov-Maxwell bracket, there are several such Casimirs [60, 61, 21]. First, the integral of any real function h_s of each distribution function f_s is preserved, i.e.,

$$\mathcal{C}_s = \int h_s(f_s) \, \mathrm{d}\mathbf{x} \, \mathrm{d}\mathbf{v}. \tag{19}$$

This family of Casimirs is a manifestation of Liouville's theorem and corresponds to conservation of phase space volume. Further we have two Casimirs related to Gauss' law (4) and the divergence-free property of the magnetic field (5),

$$\mathcal{C}_E = \int h_E(\mathbf{x}) \big(\operatorname{div} \mathbf{E} - \rho \big) \, \mathrm{d}\mathbf{x}, \tag{20}$$

$$\mathcal{C}_B = \int h_B(\mathbf{x}) \operatorname{div} \mathbf{B} \, \mathrm{d}\mathbf{x}, \tag{21}$$

where h_E and h_B are arbitrary real functions of $\mathbf{x}$. The latter functional, $\mathcal{C}_B$, is not a true Casimir but should rather be referred to as pseudo-Casimir. It acts like a Casimir in that it Poisson commutes with any other functional, but the Jacobi identity is only satisfied when $\operatorname{div} B = 0$ (see [59, 57]).

Momentum maps Φ are conserved quantities that arise from symmetries that preserve the particular Hamiltonian $\mathcal{H}$, and therefore also the equations of motion. This means that the Hamiltonian is constant along the flow of Φ, i.e.,

$$\{\mathcal{H}, \Phi\} = 0. \tag{22}$$

From Noether's theorem it follows that the generators Φ of the symmetry are preserved by the time evolution, i.e.,

$$\frac{\mathrm{d}\Phi}{\mathrm{d}t} = 0. \tag{23}$$

If the symmetry condition (22) holds, this is obvious by the antisymmetry of the Poisson bracket as

$$\frac{\mathrm{d}\Phi}{\mathrm{d}t} = \{\Phi, \mathcal{H}\} = -\{\mathcal{H}, \Phi\} = 0. \tag{24}$$

Therefore Φ is a constant of motion if and only if $\{\Phi, \mathcal{H}\} = 0$.

The complete set of constants of motion, the algebra of invariants, will be discussed elsewhere. However, as an example of a momentum map we shall consider here the total momentum

$$\mathbf{P} = \sum_s \int m_s \mathbf{v} f_s \, d\mathbf{x} \, d\mathbf{v} + \int \mathbf{E} \times \mathbf{B} \, d\mathbf{x}. \tag{25}$$

By direct computations, assuming periodic boundary conditions, it can be shown that

$$\frac{d\mathbf{P}}{dt} = \{\mathbf{P}, H\} = \int \mathbf{E}(\rho - \operatorname{div} \mathbf{E}) \, d\mathbf{x} = \int \mathbf{E} \, Q(\mathbf{x}) \, d\mathbf{x}. \tag{26}$$

defining $Q(\mathbf{x}) := \rho - \operatorname{div} \mathbf{E}$, which is a local version of the Casimir $\mathcal{C}_E$. Therefore, if at $t = 0$ the Casimir $Q \equiv 0$, then momentum is conserved. If at $t = 0$ the Casimir $Q \not\equiv 0$, then momentum is not conserved and it changes in accordance with (26). For a multi-species plasma $Q \equiv 0$ is equivalent to the physical requirement that Poisson's equation be satisfied. If for some reason it is not exactly satisfied, then we have violation of momentum conservation.

For a single species plasma, say electrons, with a neutralizing positive background charge $\rho_B(\mathbf{x})$, say ions, Poisson's equation is

$$\operatorname{div} \mathbf{E} = \rho_B - \rho_e \,. \tag{27}$$

The Poisson bracket for this case has the local Casimir

$$Q_e = \operatorname{div} \mathbf{E} + \rho_e \tag{28}$$

and it does not recognize the background charge. Because the background is stationary, the total momentum is

$$\mathbf{P} = \int m_e \mathbf{v} \, f_e \, d\mathbf{x} d\mathbf{v} + \int \mathbf{E} \times \mathbf{B} \, d\mathbf{x}, \tag{29}$$

and it satisfies

$$\frac{d\mathbf{P}_e}{dt} = \{\mathbf{P}_e, H\} = -\int \mathbf{E} \, \rho_B(\mathbf{x}) \, d\mathbf{x} \,. \tag{30}$$

3 Finite Element Exterior Calculus

Finite Element Exterior Calculus (FEEC) is a mathematical framework for mixed finite element methods, which uses geometrical and topological ideas for systematically analyzing the stability and convergence of finite element discretizations of partial differential equations. This proved to be a particularly difficult problem for Maxwell's equation, which we will use in the following as an example to review this framework.

3.1 Maxwell's Equations

When Maxwell's equations are used in some material medium, they are best understood by introducing two additional fields. The electromagnetic properties are then defined by the electric and magnetic fields, usually denoted by $\mathbf{E}$ and $\mathbf{H}$, the displacement field $\mathbf{D}$

and the magnetic induction $\mathbf{B}$. For simple materials, the electric field is related to the displacement field and the magnetic field to the magnetic induction by

$$\mathbf{D} = \varepsilon\mathbf{E}, \quad \mathbf{B} = \mu\mathbf{H},$$

where ε and μ are tensors reflecting the material properties. In vacuum they become the scalars ε_0 and μ_0, while for more complicated media such as plasmas they can be nonlinear operators [57]. The Maxwell equations with the four fields read

$$\frac{\partial \mathbf{D}}{\partial t} - \operatorname{curl}\mathbf{H} = -\mathbf{J}, \tag{31}$$

$$\frac{\partial \mathbf{B}}{\partial t} + \operatorname{curl}\mathbf{E} = 0, \tag{32}$$

$$\operatorname{div}\mathbf{D} = \rho, \tag{33}$$

$$\operatorname{div}\mathbf{B} = 0. \tag{34}$$

The mathematical interpretation of these fields become clearer when interpreting them as differential forms: $\mathbf{E}$ and $\mathbf{H}$ are 1-forms, $\mathbf{D}$ and $\mathbf{B}$ are 2-forms. The charge density ρ is a 3-form and the current density $\mathbf{J}$ a 2-form. Moreover, the electrostatic potential ϕ is a 0-form and the vector potential $\mathbf{A}$ a 1-form. The grad, curl, div operators represent the exterior derivative applied respectively to 0-forms, 1-forms and 2-forms. To be more precise, there are two kinds of differential forms, depending on the orientation. Straight differential forms have an intrinsic (or inner) orientation, whereas twisted differential forms have an outer orientation, defined by the ambient space. Faraday and div $B = 0$ are naturally inner oriented, whereas Ampère and Gauss' law are outer oriented. This knowledge can be used to define a natural discretization for Maxwell's equations. For finite difference approximations a dual mesh is needed for the discretization of twisted forms. This can already be found in Yee's scheme [81]. In the Finite Element context, only one mesh is used, but dual operators are used for the twisted forms. A detailed description of this formalism can be found in Bossavit's lecture notes [12].

3.2 Finite Element Spaces of Differential Forms

The full mathematical theory for the Finite Element discretization of differential forms is due to Arnold, Falk and Winther [2, 3] and called Finite Element Exterior Calculus (FEEC) (see also [53, 27]). Most finite element spaces appearing in this theory were known before but their connection in the context of differential forms was not made clear. The first building block of FEEC is the following commuting diagram

$$
\begin{array}{ccccccc}
H\Lambda^0(\Omega) & \xrightarrow{\ \mathsf{d}\ } & H\Lambda^1(\Omega) & \xrightarrow{\ \mathsf{d}\ } & H\Lambda^2(\Omega) & \xrightarrow{\ \mathsf{d}\ } & L^2(\Omega)^3 \\
\Big\downarrow{\Pi_0} & & \Big\downarrow{\Pi_1} & & \Big\downarrow{\Pi_2} & & \Big\downarrow{\Pi_3} \\
V_0 & \xrightarrow{\ \mathsf{d}\ } & V_1 & \xrightarrow{\ \mathsf{d}\ } & V_2 & \xrightarrow{\ \mathsf{d}\ } & V_3
\end{array}
\tag{35}
$$

where $\Omega \subset \mathbb{R}^3$, d is the exterior derivative and the Sobolev spaces of differential forms are defined by

$$H\Lambda^k(\Omega) = \{\omega \in L^2(\Lambda^k(\Omega)) \mid \mathsf{d}\omega \in L^2(\Lambda^{k+1}(\Omega))\}.$$

Obviously in a three dimensional manifold the exterior derivative of a 3-form vanishes so that $H\Lambda^3(\Omega) = L^2(\Omega)$. This diagram can also be expressed using the standard vector calculus formalism

$$
\begin{array}{ccccccc}
H^1(\Omega) & \xrightarrow{\text{grad}} & H(\text{curl},\Omega) & \xrightarrow{\text{curl}} & H(\text{div},\Omega) & \xrightarrow{\text{div}} & L^2(\Omega)^3 \\
\Big\downarrow{\Pi_0} & & \Big\downarrow{\Pi_1} & & \Big\downarrow{\Pi_2} & & \Big\downarrow{\Pi_3} \\
V_0 & \xrightarrow{\text{grad}} & V_1 & \xrightarrow{\text{curl}} & V_2 & \xrightarrow{\text{div}} & V_3
\end{array}
\tag{36}
$$

The first row of (36) represents the exact sequence of function spaces involved in Maxwell's equations in the sense that at each node, the kernel of the next operator is the image of the previous: Im(grad) = Ker(curl), Im(curl) = Ker(div). And the power of the conforming Finite Element framework is that this exact sequence can be reproduced at the discrete level by choosing the appropriate discrete spaces. The order of the approximation is dictated by the choice made for V_0 and the requirement of having an exact sequence at the discrete level. The projection operators Π_i are the Finite Element interpolants, which have the property that the diagram is commuting. This means for example, that the grad of the projection on V_0 is identical to the projection of the grad on V_0. As proven by Arnold, Falk and Winther, their choice of Finite Elements naturally leads to stable discretizations.

There are many known sequences of Finite Element spaces fitting in this diagram. The sequences proposed by Arnold, Falk and Winther are based on well known Finite Element spaces: on tetrahedra these are H^1 conforming $\mathbb{P}_k$ Lagrange Finite Elements for V_0, the $H(\text{curl})$ conforming Nédélec elements for V_1, the $H(\text{div})$ conforming Raviart-Thomas elements for V_2 and Discontinuous Galerkin elements for V_3. A similar sequence can be defined on hexahedra based on the H^1 conforming $\mathbb{Q}_k$ Lagrange Finite Elements for V_0.

Other such exact sequences are available. Let us in particular cite the mimetic spectral elements [46, 38, 65] and the spline finite elements [14, 15, 67], that we shall use in this work, as splines are generally favoured in PIC codes due to of their smoothness properties, which enable noise reduction.

3.3 Finite Element discretization of Maxwell's Equations

This framework is enough to express discrete relations between all the straight (or primal forms) *i.e.* **E**, **B**, **A** and ϕ. The commuting diagram yields a direct expression of the discrete Faraday equation. Indeed projecting all the components of the equation onto V_2 yields

$$
\frac{\partial \Pi_2 \mathbf{B}}{\partial t} + \Pi_2 \operatorname{curl} \mathbf{E} = 0,
$$

which is equivalent due to the commuting diagram property to

$$
\frac{\partial \Pi_2 \mathbf{B}}{\partial t} + \operatorname{curl} \Pi_1 \mathbf{E} = 0.
$$

Denoting with an h index the discrete fields, $\mathbf{B}_h = \Pi_2 \mathbf{B}$, $\mathbf{E}_h = \Pi_1 \mathbf{E}$, this yields the discrete Faraday equation,

$$
\frac{\partial \mathbf{B}_h}{\partial t} + \operatorname{curl} \mathbf{E}_h = 0.
\tag{37}
$$

In the same way, the discrete electric and magnetic fields are defined exactly as in the continuous case from the discrete potentials thanks to the compatible Finite Element spaces,

$$\mathbf{E}_h = \Pi_1 \mathbf{E} = -\Pi_1 \operatorname{grad} \phi - \Pi_1 \frac{\partial \mathbf{A}}{\partial t} = -\operatorname{grad} \Pi_0 \phi - \frac{\partial \Pi_1 \mathbf{A}}{\partial t} = -\operatorname{grad} \phi_h - \frac{\partial \mathbf{A}_h}{\partial t}, \quad (38)$$

$$\mathbf{B}_h = \Pi_2 \mathbf{B} = \Pi_2 \operatorname{curl} \mathbf{A} = \operatorname{curl} \Pi_1 \mathbf{A} = \operatorname{curl} \mathbf{A}_h, \quad (39)$$

so that automatically we get

$$\operatorname{div} \mathbf{B}_h = 0. \quad (40)$$

On the other hand, the Ampère equation and Gauss' law relate expressions involving twisted differential forms. In the Finite Element framework, these should be expressed on the dual complex, which inherits the commuting diagram properties from the primal complex:

$$
\begin{array}{ccccccc}
L^2(\Omega)^3 & \xrightarrow{\operatorname{div}^*} & (H(\operatorname{div}, \Omega))^* & \xrightarrow{\operatorname{curl}^*} & (H(\operatorname{curl}, \Omega))^* & \xrightarrow{\operatorname{grad}^*} & (H^1(\Omega))^* \\
\Pi_0 \downarrow & & \Pi_1 \downarrow & & \Pi_2 \downarrow & & \Pi_3 \downarrow \\
V_0^* & \xrightarrow{\operatorname{div}^*} & V_1^* & \xrightarrow{\operatorname{curl}^*} & V_2^* & \xrightarrow{\operatorname{grad}^*} & V_3^*
\end{array}
\quad (41)
$$

Recalling that the dual operator denoted by T^* of an operator T in $L^2(\Omega)$ is defined, using a test function v by $\int_\Omega T^* u \, v \, d\mathbf{x} = \int_\Omega u \, T v \, d\mathbf{x}$, we find

$$\int_\Omega \operatorname{grad}^* \mathbf{u} \, \varphi \, d\mathbf{x} = \int_\Omega \mathbf{u} \cdot \operatorname{grad} \varphi \, d\mathbf{x} = -\int_\Omega \operatorname{div} \mathbf{u} \cdot \varphi \, d\mathbf{x} \quad (42)$$

using the Green formula and assuming periodic boundary conditions, so that $\operatorname{grad}^* = -\operatorname{div}$. In the same way

$$\int_\Omega \operatorname{curl}^* \mathbf{u} \cdot \mathbf{v} \, d\mathbf{x} = \int_\Omega \mathbf{u} \cdot \operatorname{curl} \mathbf{v} \, d\mathbf{x} = \int_\Omega \operatorname{curl} \mathbf{u} \cdot \mathbf{v} \, d\mathbf{x}, \quad (43)$$

so that $\operatorname{curl}^* = \operatorname{curl}$. Due to these properties the discrete dual spaces are such that $V_0^* = V_3$, $V_1^* = V_2$, $V_2^* = V_1$ and $V_3^* = V_0$.

In the finite element framework the dual operators and spaces are not explicitly needed. They are most naturally used seamlessly by keeping the weak formulation of the corresponding equations. The weak form of Ampère's equation is found by taking the dot product of (2) with a test function $\mathbf{F}$ and applying a Green formula, which corresponds to integration by parts. Assuming periodic boundary conditions, the weak solution of the Ampère equation is:

Find $(\mathbf{E}, \mathbf{B}) \in H(\operatorname{curl}, \Omega) \times H(\operatorname{div}, \Omega)$ such that

$$\frac{d}{dt} \int_\Omega \mathbf{E} \cdot \mathbf{F} \, d\mathbf{x} - c^2 \int_\Omega \mathbf{B} \cdot \operatorname{curl} \mathbf{F} \, d\mathbf{x} = -\frac{1}{\varepsilon_0} \int_\Omega \mathbf{J} \cdot \mathbf{F} \, d\mathbf{x} \quad \forall \mathbf{F} \in H(\operatorname{curl}, \Omega). \quad (44)$$

The discrete version is obtained by replacing the continuous spaces by their finite dimensional subspace, which yields the discrete weak Ampère equation:

Find $(\mathbf{E}_h, \mathbf{B}_h) \in V_1 \times V_2$ such that

$$\frac{d}{dt} \int_\Omega \mathbf{E}_h \cdot \mathbf{F}_h \, d\mathbf{x} - c^2 \int_\Omega \mathbf{B}_h \cdot \operatorname{curl} \mathbf{F}_h \, d\mathbf{x} = -\frac{1}{\varepsilon_0} \int_\Omega \mathbf{J}_h \cdot \mathbf{F}_h \, d\mathbf{x} \quad \forall \mathbf{F}_h \in V_1. \quad (45)$$

In the same way the weak form of Gauss' law reads:
Find $\mathbf{E} \in H(\text{curl}, \Omega)$ such that

$$\int_\Omega \mathbf{E} \cdot \nabla \varphi \, d\mathbf{x} = -\frac{1}{\varepsilon_0} \int_\Omega \rho \varphi \, d\mathbf{x} \quad \forall \varphi \in H^1(\Omega), \tag{46}$$

its discrete version being:
Find $\mathbf{E}_h \in V_1$ such that

$$\int_\Omega \mathbf{E}_h \cdot \nabla \varphi_h \, d\mathbf{x} = -\frac{1}{\varepsilon_0} \int_\Omega \rho_h \varphi_h \, d\mathbf{x} \quad \forall \varphi_h \in V_0. \tag{47}$$

The last step for the Finite Element discretization is to define a basis for each of the finite dimensional spaces V_0, V_1, V_2, V_3, with $\dim V_k = N_k$ and to find equations relating the coefficients on these bases. Let us denote by $\{\Lambda_i^0\}_{i=1\ldots N_0}$ and $\{\Lambda_i^3\}_{i=1\ldots N_3}$ a basis of V_0 and V_3 respectively which are spaces of scalar functions, and $\{\mathbf{\Lambda}_i^1\}_{i=1\ldots N_1}$ a basis of $V_1 \subset H(\text{curl}, \Omega)$ and $\{\mathbf{\Lambda}_i^2\}_{i=1\ldots N_2}$ a basis of $V_2 \subset H(\text{div}, \Omega)$, which are vector valued functions. We shall also need for each basis Λ_i^k the dual basis denoted by σ_i^k defined by $\sigma_i^k(\Lambda_j^k) = \delta_{ij}$, where δ_{ij} is the Kronecker symbol, whose value is one for $i = j$ and zero else. The dual basis corresponds to the degrees of freedom in the Finite Element terminology.

We can write elements of V_1 and V_2, respectively, as

$$\mathbf{E}_h = \sum_{i=1}^{N_1} e_i \mathbf{\Lambda}_i^1, \qquad \mathbf{B}_h = \sum_{i=1}^{N_2} b_i \mathbf{\Lambda}_i^2, \tag{48}$$

denoting by $\mathbf{e} = (e_1, \ldots, e_{N_1})^\top$ and $\mathbf{b} = (b_1, \ldots, b_{N_2})^\top$ the corresponding degrees of freedom, with $e_i = \sigma_i^1(\mathbf{E}_h)$ and $b_i = \sigma_i^2(\mathbf{B}_h)$. Due to the exact sequence property we have that $\text{curl}\, \mathbf{E}_h \in V_2$ for all $\mathbf{E}_h \in V_1$, so that $\text{curl}\, \mathbf{E}_h$ can be expressed in the basis of V_2 by

$$\text{curl}\, \mathbf{E}_h = \sum_{i=1}^{N_2} c_i \mathbf{\Lambda}_i^2.$$

Let us also denote by $\mathbf{c} = (c_1, \ldots, c_{N_2})^\top$. On the other hand

$$\text{curl}\, \mathbf{E}_h = \text{curl}\left(\sum_{j=1}^{N_1} e_i \mathbf{\Lambda}_j^1\right) = \sum_{j=1}^{N_1} e_j \, \text{curl}\, \mathbf{\Lambda}_j^1, \qquad \sigma_i^2(\text{curl}\, \mathbf{E}_h) = \sum_{j=1}^{N_1} e_j \sigma_i^2(\text{curl}\, \mathbf{\Lambda}_j^1).$$

Denoting by $\mathbb{C}$ the discrete curl matrix,

$$\mathbb{C} = (\sigma_i^2(\text{curl}\, \mathbf{\Lambda}_j^1))_{1 \leq i \leq N_2, 1 \leq j \leq N_1}, \tag{49}$$

the degrees of freedom of $\text{curl}\, \mathbf{E}_h$ in V_2 are related to the degrees of freedom of $\mathbf{E}_h$ in V_1 by $\mathbf{c} = \mathbb{C}\mathbf{e}$. In the same way we can define the discrete gradient matrix $\mathbb{G}$ and the discrete divergence matrix $\mathbb{D}$, given by

$$\mathbb{G} = (\sigma_i^1(\text{grad}\, \Lambda_j^0))_{1 \leq i \leq N_1, 1 \leq j \leq N_0} \quad \text{and} \quad \mathbb{D} = (\sigma_i^3(\text{div}\, \mathbf{\Lambda}_j^2))_{1 \leq i \leq N_3, 1 \leq j \leq N_2}, \tag{50}$$

respectively. Denoting by $\boldsymbol{\varphi} = (\varphi_1, \ldots, \varphi_{N_0})^\top$ and $\mathbf{a} = (a_1, \ldots, a_{N_1})^\top$ the degrees of freedom of the potentials ϕ_h and $\mathbf{A}_h$, with $\varphi_i = \sigma_i^0(\phi_h)$ and $a_i = \sigma_i^1(\mathbf{A}_h)$, the relation (38)

between the discrete fields (48) and the potentials can be written using only the degrees of freedom as

$$\mathbf{e} = -\mathbb{G}\boldsymbol{\varphi} - \frac{\mathrm{d}\mathbf{a}}{\mathrm{d}t}, \qquad \mathbf{b} = \mathbb{C}\mathbf{a}. \tag{51}$$

Finally, we need the mass matrices in each of the discrete spaces V_i, which define the discrete Hodge operator linking the primal exact sequence with the dual exact sequence. We denote by $(M_1)_{i,j} = \int_\Omega \boldsymbol{\Lambda}_i^1 \cdot \boldsymbol{\Lambda}_j^1 \, \mathrm{d}\mathbf{x}$ the mass matrix in V_1 and similarly M_0, M_2, M_3 the mass matrices in V_0, V_2 and V_3, respectively. Using these definitions as well as $\boldsymbol{\varrho} = (\varrho_1, \ldots, \varrho_{N_0})^\top$ and $\mathbf{j} = (j_1, \ldots, j_{N_2})^\top$ with $\varrho_i = \sigma_i^0(\rho_h)$ and $j_i = \sigma_i^2(\mathbf{J}_h)$, we obtain a system of ordinary differential equations for each of the continuous equations, namely

$$M_1 \frac{\mathrm{d}\mathbf{e}}{\mathrm{d}t} - \mathbb{C}^\top M_2 \mathbf{b} = -\mathbf{j}, \tag{52}$$

$$\frac{\mathrm{d}\mathbf{b}}{\mathrm{d}t} + \mathbb{C}\mathbf{e} = 0, \tag{53}$$

$$\mathbb{G}^\top M_1 \mathbf{e} = \frac{\boldsymbol{\varrho}}{\varepsilon_0}, \tag{54}$$

$$\mathbb{D}\mathbf{b} = 0. \tag{55}$$

Moreover the exact sequence properties can also be expressed at the matrix level. The primal sequence being

$$\mathbb{R}^{N_0} \xrightarrow{\ \mathbb{G}\ } \mathbb{R}^{N_1} \xrightarrow{\ \mathbb{C}\ } \mathbb{R}^{N_2} \xrightarrow{\ \mathbb{D}\ } \mathbb{R}^{N_3}, \tag{56}$$

with $\operatorname{Im}\mathbb{G} = \operatorname{Ker}\mathbb{C}$, $\operatorname{Im}\mathbb{C} = \operatorname{Ker}\mathbb{D}$, and the dual sequence being

$$\mathbb{R}^{N_3} \xrightarrow{\ \mathbb{D}^\top\ } \mathbb{R}^{N_2} \xrightarrow{\ \mathbb{C}^\top\ } \mathbb{R}^{N_1} \xrightarrow{\ \mathbb{G}^\top\ } \mathbb{R}^{N_0}, \tag{57}$$

with $\operatorname{Im}\mathbb{D}^\top = \operatorname{Ker}\mathbb{C}^\top$, $\operatorname{Im}\mathbb{C}^\top = \operatorname{Ker}\mathbb{G}^\top$.

4 Discretization of the Hamiltonian Structure

The continuous bracket (8) relies on a Eulerian (as opposed to Lagrangian) formulation of the Vlasov equation: the functionals on which the bracket depends are the distribution function f in addition to the electric and magnetic fields $\mathbf{E}$ and $\mathbf{B}$. A natural discretization relies on selecting a finite number of characteristics instead of the continuum particle distribution function. A natural way to do this is to replace f by $f_h(\mathbf{x}, \mathbf{v}) = \sum_a w_a \, \delta(\mathbf{x} - \mathbf{x}_a(t)) \, \delta(\mathbf{v} - \mathbf{v}_a(t))$, which amounts to a Monte Carlo discretization of the first three integrals in (8) if the initial phase space positions $(\mathbf{x}_a(0), \mathbf{v}_a(0))$ are randomly drawn. Moreover instead of allowing the fields $\mathbf{E}$ and $\mathbf{B}$ to vary in $H(\operatorname{curl}, \Omega)$ and $H(\operatorname{div}, \Omega)$ respectively, we keep them in the discrete subspaces V_1 and V_2. This procedure yields a discrete Poisson bracket, from which one obtains the dynamics of a finite (large) number of scalars: the particle phase space positions and the coefficients of the fields in the Finite Element basis, where we denote by e_i the degrees of freedom for $\mathbf{E}_h$ and by b_i the degrees of freedom for $\mathbf{B}_h$. Further, $\mathbf{z}_a(t) = (\mathbf{x}_a, \mathbf{v}_a)$ denotes the phase space position at time t of the particle that was at $\mathbf{z}_{k,0}$ at time t_0. The FEEC framework introduced in the previous section automatically provides the following discretization spaces for the potentials and the fields

$$\phi_h \in V_0, \quad \mathbf{A}_h, \mathbf{E}_h \in V_1, \quad \mathbf{B}_h \in V_2.$$

The coefficient vectors of the fields are denoted $\mathbf{e}$ and $\mathbf{b}$. In order to also get a vector expression for the particle quantities, we denote by

$$\mathbf{X} = (\mathbf{x}_1, \ldots, \mathbf{x}_{N_p})^\top, \qquad \mathbf{V} = (\mathbf{v}_1, \ldots, \mathbf{v}_{N_p})^\top. \tag{58}$$

We now want to transform (8) into a discrete Poisson bracket for the dynamics of the coefficients $\mathbf{e}$, $\mathbf{b}$, $\mathbf{X}$ and $\mathbf{V}$.

4.1   discretization of the Functional Field Derivatives

Upon inserting (48), any functional $F[\mathbf{E}_h]$ can be considered as a function $\hat{F}(\mathbf{e})$ of the finite element coefficients,

$$F[\mathbf{E}_h] = \hat{F}(\mathbf{e}). \tag{59}$$

Therefore, we can write the functional derivative as

$$\left\langle \frac{\delta F[\mathbf{E}_h]}{\delta \mathbf{E}}, \bar{\mathbf{E}}_h \right\rangle_{L^2} = \left\langle \frac{\partial \hat{F}(\mathbf{e})}{\partial \mathbf{e}}, \bar{\mathbf{e}} \right\rangle_{\mathbb{R}^{N_1}}, \tag{60}$$

with

$$\bar{\mathbf{E}}_h(\mathbf{x}) = \sum_{i=1}^{N_1} \bar{e}_i(t)\, \boldsymbol{\Lambda}_i^1(\mathbf{x}), \qquad\qquad \bar{\mathbf{e}} = (\bar{e}_1, \ldots, \bar{e}_{N_1})^\top. \tag{61}$$

Expressing the functional derivative on the dual basis $\tilde{\boldsymbol{\Lambda}}_i^1(\mathbf{x})$ of $\boldsymbol{\Lambda}_i^1(\mathbf{x})$, such that $\int \boldsymbol{\Lambda}_i^1(\mathbf{x}) \cdot \tilde{\boldsymbol{\Lambda}}_j^1(\mathbf{x})\, \mathrm{d}\mathbf{x} = \delta_{ij}$ we find using (60) for $\bar{\mathbf{E}}_h = \boldsymbol{\Lambda}_i^1(\mathbf{x})$ that

$$\frac{\delta F[\mathbf{E}_h]}{\delta \mathbf{E}} = \sum_{i=1}^{N_1} \frac{\partial \hat{F}(\mathbf{e})}{\partial e_i} \tilde{\boldsymbol{\Lambda}}_i^1(\mathbf{x}). \tag{62}$$

On the other hand expanding on the original basis

$$\tilde{\boldsymbol{\Lambda}}_i^1(\mathbf{x}) = \sum_{j=1}^{N_1} a_{ij} \boldsymbol{\Lambda}_i^1(\mathbf{x}) \tag{63}$$

and taking the L^2 inner product with $\boldsymbol{\Lambda}_i^1(\mathbf{x})$ we find that the matrix $A = (a_{ij})$ verifies $AM_1 = \mathbb{I}_{N_1}$ so that A is the inverse of the mass matrix M_1. so that

$$\frac{\delta F[\mathbf{E}_h]}{\delta \mathbf{E}} = \sum_{i,j=1}^{N_1} \frac{\partial \hat{F}(\mathbf{e})}{\partial e_i} (M_1^{-1})_{ij}\, \boldsymbol{\Lambda}_j^1(\mathbf{x}). \tag{64}$$

In full analogy we find

$$\frac{\delta F[\mathbf{B}_h]}{\delta \mathbf{B}} = \sum_{i,j=1}^{N_2} \frac{\partial \hat{F}(\mathbf{b})}{\partial b_i} (M_2^{-1})_{ij}\, \boldsymbol{\Lambda}_j^2(\mathbf{x}). \tag{65}$$

Next, using (49), we find

$$\text{curl}\, \frac{\delta F[\mathbf{E}_h]}{\delta \mathbf{E}} = \sum_{i,j=1}^{N_1} \frac{\partial \hat{F}(\mathbf{e})}{\partial e_i}\, (M_1^{-1})_{ij} \mathbb{C}_{jk}\, \mathbf{\Lambda}_k^2(\mathbf{x}). \tag{66}$$

Finally, we can express the term in bracket

$$\int \text{curl}\, \frac{\delta F[\mathbf{E}_h]}{\delta \mathbf{E}} \cdot \frac{\delta G[\mathbf{B}_h]}{\delta \mathbf{B}}\, \mathrm{d}\mathbf{x} = \tag{67}$$

$$\sum_{i,j=1}^{N_1} \sum_{k=1}^{N_2} \sum_{m,n=1}^{N_2} \frac{\partial \hat{F}(\mathbf{e})}{\partial e_i}\, (M_1^{-1})_{ij} \mathbb{C}_{jk} \frac{\partial \hat{G}(\mathbf{b})}{\partial b_m}\, (M_2^{-1})_{mn} \int \mathbf{\Lambda}_k^2(\mathbf{x}) \cdot \mathbf{\Lambda}_n^2(\mathbf{x})\, \mathrm{d}\mathbf{x} \tag{68}$$

$$= \sum_{i,j=1}^{N_1} \sum_{k=1}^{N_2} \frac{\partial \hat{F}(\mathbf{e})}{\partial e_i}\, (M_1^{-1})_{ij} \mathbb{C}_{jk} \frac{\partial \hat{G}(\mathbf{b})}{\partial b_k} = \sum_{i=1}^{N_1} \sum_{k=1}^{N_2} \frac{\partial \hat{F}(\mathbf{e})}{\partial e_i}\, (M_1^{-1}\mathbb{C})_{ik} \frac{\partial \hat{G}(\mathbf{b})}{\partial b_k} \tag{69}$$

The symmetric term in the bracket is handled similarly. In the next step we need to discretise the distribution function f and the corresponding functional derivatives.

4.2   discretization of the Functional Particle Derivatives

We proceed by assuming a particle-like distribution function for N_p particles labeled by a,

$$f_h(\mathbf{x}, \mathbf{v}, t) = \sum_{a=1}^{N_p} w_a\, \delta\big(\mathbf{x} - \mathbf{x}_a(t)\big)\, \delta\big(\mathbf{v} - \mathbf{v}_a(t)\big), \tag{70}$$

with mass m_a, charge q_a, weights w_a, particle positions $\mathbf{x}_a$ and particle velocities $\mathbf{v}_a$. Functionals of the distribution function, $F[f]$, can be considered as functions of the particle phase space trajectories $(\mathbf{X}, \mathbf{V})$ upon inserting (70),

$$F[f_h] = \hat{F}(\mathbf{X}, \mathbf{V}). \tag{71}$$

Variation gives,

$$\delta \hat{F}(\mathbf{X}, \mathbf{V}) = \sum_{a=1}^{N_p} \left(\frac{\partial \hat{F}}{\partial \mathbf{x}_a}\, \delta \mathbf{x}_a + \frac{\partial \hat{F}}{\partial \mathbf{v}_a}\, \delta \mathbf{v}_a \right)$$

$$= \int \frac{\delta F}{\delta f}\, \delta f\, \mathrm{d}\mathbf{x}\, \mathrm{d}\mathbf{v}$$

$$= -\sum_{a=1}^{N_p} w_a \int \frac{\delta F}{\delta f} \bigg(\delta\big(\mathbf{v} - \mathbf{v}_a(t)\big)\, \frac{\partial}{\partial \mathbf{x}} \delta\big(\mathbf{x} - \mathbf{x}_a(t)\big) \cdot \delta \mathbf{x}_a$$

$$+ \delta\big(\mathbf{x} - \mathbf{x}_a(t)\big)\, \frac{\partial}{\partial \mathbf{v}} \delta\big(\mathbf{v} - \mathbf{v}_a(t)\big) \cdot \delta \mathbf{v}_a \bigg)\, \mathrm{d}\mathbf{x}\, \mathrm{d}\mathbf{v}$$

$$= \sum_{a=1}^{N_p} w_a \left(\frac{\partial}{\partial \mathbf{x}} \frac{\delta F}{\delta f} \bigg|_{(\mathbf{x}_a, \mathbf{v}_a)} \cdot \delta \mathbf{x}_a + \frac{\partial}{\partial \mathbf{v}} \frac{\delta F}{\delta f} \bigg|_{(\mathbf{x}_a, \mathbf{v}_a)} \cdot \delta \mathbf{v}_a \right). \tag{72}$$

Upon equating the second and last terms, we obtain

$$\frac{\partial \hat{F}}{\partial \mathbf{x}_a} = w_a \frac{\partial}{\partial \mathbf{x}} \frac{\delta F}{\delta f} \bigg|_{(\mathbf{x}_a, \mathbf{v}_a)} \qquad \text{and} \qquad \frac{\partial \hat{F}}{\partial \mathbf{v}_a} = w_a \frac{\partial}{\partial \mathbf{v}} \frac{\delta F}{\delta f} \bigg|_{(\mathbf{x}_a, \mathbf{v}_a)}. \tag{73}$$

Now we have all the ingredients necessary to perform the spatial discretization of the Poisson bracket.

4.3 Discrete Poisson Bracket

Replacing all functional derivatives in (8) as outlined in the previous two sections, we obtain the semi-discrete Poisson bracket

$$
\begin{aligned}
\{\hat{F}, \hat{G}\}[\mathbf{X}, \mathbf{V}, \mathbf{e}, \mathbf{b}] = & \sum_a \frac{1}{m_a w_a} \left(\frac{\partial \hat{F}}{\partial \mathbf{x}_a} \cdot \frac{\partial \hat{G}}{\partial \mathbf{v}_a} - \frac{\partial \hat{G}}{\partial \mathbf{x}_a} \cdot \frac{\partial \hat{F}}{\partial \mathbf{v}_a} \right) \\
& + \sum_{a=1}^{N_p} \sum_{i,j=1}^{N_1} \frac{q_a}{m_a w_a} \left(\frac{\partial \hat{G}}{\partial e_i} (M_1^{-1})_{ij} \, \mathbf{\Lambda}_j^1(\mathbf{x}_a) \cdot \frac{\partial \hat{F}}{\partial \mathbf{v}_a} - \frac{\partial \hat{F}}{\partial e_i} (M_1^{-1})_{ij} \, \mathbf{\Lambda}_j^1(\mathbf{x}_a) \cdot \frac{\partial \hat{G}}{\partial \mathbf{v}_a} \right) \\
& + \sum_{a=1}^{N_p} \sum_{i=1}^{N_2} \frac{q_a}{m_a^2 w_a^2} b_i(t) \, \mathbf{\Lambda}_i^2(\mathbf{x}_a) \cdot \left(\frac{\partial \hat{F}}{\partial \mathbf{v}_a} \times \frac{\partial \hat{G}}{\partial \mathbf{v}_a} \right) \\
& + \sum_{i,j=1}^{N_1} \sum_{k,l=1}^{N_2} \left(\frac{\partial \hat{F}}{\partial e_i} (M_1^{-1})_{ij} \, \mathbb{C}_{jk}^\top (M_2^{-1})_{kl} \frac{\partial \hat{G}}{\partial b_l} - \frac{\partial \hat{G}}{\partial e_i} (M_1^{-1})_{ij} \, \mathbb{C}_{jk}^\top (M_2^{-1})_{kl} \frac{\partial \hat{F}}{\partial b_l} \right), \quad (74)
\end{aligned}
$$

with the curl matrix $\mathbb{C}$ as given in (49). Here and in the following, we do not distinguish between particles of different species. As each particle labeled by a is carrying its own mass m_a and charge q_a, the separation into different species would be redundant.

In order to express the semi-discrete Poisson bracket (74) in matrix form, we denote by $\mathbb{\Lambda}^1(\mathbf{X})$ the $3N_p \times N_1$ matrix with generic term $\mathbf{\Lambda}_i^1(\mathbf{x}_a)$, where $1 \leq a \leq N_p$ and $1 \leq i \leq N_1$, and by $\mathbb{B}(\mathbf{X}, \mathbf{b})$ the $3N_p \times 3N_p$ block diagonal matrix with generic block

$$
\widehat{\mathbf{B}}_h(\mathbf{x}_a, t) = \sum_{i=1}^{N_2} b_i(t) \begin{pmatrix} 0 & \Lambda_i^{2,3}(\mathbf{x}_a) & -\Lambda_i^{2,2}(\mathbf{x}_a) \\ -\Lambda_i^{2,3}(\mathbf{x}_a) & 0 & \Lambda_i^{2,1}(\mathbf{x}_a) \\ \Lambda_i^{2,2}(\mathbf{x}_a) & -\Lambda_i^{2,1}(\mathbf{x}_a) & 0 \end{pmatrix}. \quad (75)
$$

Further, let us introduce a mass matrix M_p and a charge matrix M_q for the particles. Both are diagonal $N_p \times N_p$ matrices with elements $(M_p)_{aa} = m_a w_a$ and $(M_q)_{aa} = q_a$, respectively. Additionally, we will need the $3N_p \times 3N_p$ matrices

$$
\mathbb{M}_p = M_p \otimes \mathbb{1}_{3 \times 3}, \qquad \mathbb{M}_q = M_q \otimes \mathbb{1}_{3 \times 3}, \quad (76)
$$

where $\mathbb{1}_{3 \times 3}$ denotes the 3×3 identity matrix. This allows us to rewrite

$$
\begin{aligned}
\sum_{a=1}^{N_p} \sum_{i=1}^{N_2} \frac{q_a}{m_a^2 w_a^2} b_i(t) \, \mathbf{\Lambda}_i^2(\mathbf{x}_a) \cdot \left(\frac{\partial \hat{F}}{\partial \mathbf{v}_a} \times \frac{\partial \hat{G}}{\partial \mathbf{v}_a} \right) = & \\
= -\sum_{a=1}^{N_p} \frac{\partial \hat{F}}{\partial \mathbf{v}_a} \frac{q_a}{m_a w_a} \cdot \sum_{i=1}^{N_2} b_i(t) \, \mathbf{\Lambda}_i^2(\mathbf{x}_a) & \times \frac{1}{m_a w_a} \frac{\partial \hat{G}}{\partial \mathbf{v}_a} \\
= -\left(\frac{\partial \hat{F}}{\partial \mathbf{V}} \right)^\top \mathbb{M}_p^{-1} \mathbb{M}_q \mathbb{B}(\mathbf{X}, \mathbf{b}) \, \mathbb{M}_p^{-1} & \left(\frac{\partial \hat{G}}{\partial \mathbf{V}} \right). \quad (77)
\end{aligned}
$$

Here, the derivatives are represented by the $3N_p$ vector

$$
\frac{\partial \hat{F}}{\partial \mathbf{V}} = \left(\frac{\partial \hat{F}}{\partial \mathbf{v}_1}, \dots, \frac{\partial \hat{F}}{\partial \mathbf{v}_{N_p}} \right)^\top = \left(\frac{\partial \hat{F}}{\partial \mathrm{v}_1^1}, \frac{\partial \hat{F}}{\partial \mathrm{v}_1^2}, \frac{\partial \hat{F}}{\partial \mathrm{v}_1^3}, \dots, \frac{\partial \hat{F}}{\partial \mathrm{v}_{N_p}^1}, \frac{\partial \hat{F}}{\partial \mathrm{v}_{N_p}^2}, \frac{\partial \hat{F}}{\partial \mathrm{v}_{N_p}^3} \right)^\top, \quad (78)
$$

and correspondingly for $\partial \hat{G}/\partial \mathbf{V}$, $\partial \hat{F}/\partial \mathbf{e}$, $\partial \hat{F}/\partial \mathbf{b}$, etc.. With that, the discrete Poisson bracket (74) becomes

$$
\begin{aligned}
\{\hat{F}, \hat{G}\}[\mathbf{X}, \mathbf{V}, \mathbf{e}, \mathbf{b}] =\ & \frac{\partial \hat{F}}{\partial \mathbf{X}} \mathbb{M}_p^{-1} \frac{\partial \hat{G}}{\partial \mathbf{V}} - \frac{\partial \hat{G}}{\partial \mathbf{X}} \mathbb{M}_p^{-1} \frac{\partial \hat{F}}{\partial \mathbf{V}} \\
& + \left(\frac{\partial \hat{F}}{\partial \mathbf{V}}\right)^{\top} \mathbb{M}_p^{-1} \mathbb{M}_q \mathbb{A}^1(\mathbf{X})^{\top} M_1^{-1} \left(\frac{\partial \hat{G}}{\partial \mathbf{e}}\right) \\
& - \left(\frac{\partial \hat{F}}{\partial \mathbf{e}}\right)^{\top} M_1^{-1} \mathbb{A}^1(\mathbf{X}) \, \mathbb{M}_q \mathbb{M}_p^{-1} \left(\frac{\partial \hat{G}}{\partial \mathbf{V}}\right) \\
& + \left(\frac{\partial \hat{F}}{\partial \mathbf{V}}\right)^{\top} \mathbb{M}_p^{-1} \mathbb{M}_q \mathbb{B}(\mathbf{X}, \mathbf{b}) \, \mathbb{M}_p^{-1} \left(\frac{\partial \hat{G}}{\partial \mathbf{V}}\right) \\
& + \left(\frac{\partial \hat{F}}{\partial \mathbf{e}}\right)^{\top} M_1^{-1} \mathbb{C}^{\top} \left(\frac{\partial \hat{G}}{\partial \mathbf{b}}\right) - \left(\frac{\partial \hat{F}}{\partial \mathbf{b}}\right)^{\top} \mathbb{C} M_1^{-1} \left(\frac{\partial \hat{G}}{\partial \mathbf{e}}\right). \quad (79)
\end{aligned}
$$

The action of this bracket on two functionals $\hat{F}$ and $\hat{G}$ can also be expressed as

$$
\{\hat{F}, \hat{G}\} = \mathrm{D}\hat{F}^{\top} \mathcal{J}(\mathbf{u}) \, \mathrm{D}\hat{G},
$$

denoting by D the derivative with respect to the dynamical variables $\mathbf{u}$ with $\mathbf{u} = (\mathbf{X}, \mathbf{V}, \mathbf{e}, \mathbf{b})$ and by $\mathcal{J}$ the Poisson matrix, given by

$$
\mathcal{J}(\mathbf{u}) = \begin{pmatrix}
0 & \mathbb{M}_p^{-1} & 0 & 0 \\
-\mathbb{M}_p^{-1} & \mathbb{M}_p^{-1} \mathbb{M}_q \mathbb{B}(\mathbf{X}, \mathbf{b}) \, \mathbb{M}_p^{-1} & \mathbb{M}_p^{-1} \mathbb{M}_q \mathbb{A}^1(\mathbf{X}) M_1^{-1} & 0 \\
0 & -M_1^{-1} \mathbb{A}^1(\mathbf{X})^{\top} \mathbb{M}_q \mathbb{M}_p^{-1} & 0 & M_1^{-1} \mathbb{C}^{\top} \\
0 & 0 & -\mathbb{C} M_1^{-1} & 0
\end{pmatrix}. \quad (80)
$$

We immediately see that $\mathcal{J}(\mathbf{u})$ is anti-symmetric, but we have to show that it satisfies the Jacobi identity.

4.4 Jacobi Identity

In order to prove that the discrete Poisson bracket (79) satisfies the Jacobi identity, we have to show that the following condition is satisfied (see e.g. [56, Section IV] or [39, Section VII.2, Lemma 2.3]),

$$
\sum_l \left(\frac{\partial \mathcal{J}_{ij}(\mathbf{u})}{\partial \mathrm{u}_l} \mathcal{J}_{lk}(\mathbf{u}) + \frac{\partial \mathcal{J}_{jk}(\mathbf{u})}{\partial \mathrm{u}_l} \mathcal{J}_{li}(\mathbf{u}) + \frac{\partial \mathcal{J}_{ki}(\mathbf{u})}{\partial \mathrm{u}_l} \mathcal{J}_{lj}(\mathbf{u}) \right) = 0 \quad \text{for all} \quad i, j, k. \quad (81)
$$

To simplify the verification of this identity, we start with identifying those blocks of the Poisson matrix $\mathcal{J}$ whose elements contribute to the above condition. Therefore, we write

$$
\mathcal{J}(\mathbf{u}) = \begin{pmatrix}
J_{11}(\mathbf{u}) & J_{12}(\mathbf{u}) & J_{13}(\mathbf{u}) & J_{14}(\mathbf{u}) \\
J_{21}(\mathbf{u}) & J_{22}(\mathbf{u}) & J_{23}(\mathbf{u}) & J_{24}(\mathbf{u}) \\
J_{31}(\mathbf{u}) & J_{32}(\mathbf{u}) & J_{33}(\mathbf{u}) & J_{34}(\mathbf{u}) \\
J_{41}(\mathbf{u}) & J_{42}(\mathbf{u}) & J_{43}(\mathbf{u}) & J_{44}(\mathbf{u})
\end{pmatrix} \quad \text{and} \quad \mathbf{u} = \begin{pmatrix} \mathbf{X} \\ \mathbf{V} \\ \mathbf{e} \\ \mathbf{b} \end{pmatrix}. \quad (82)
$$

The Poisson matrix $\mathcal{J}$ only depends on $\mathbf{X}$ and $\mathbf{b}$, so in (81) we have to sum l only over the corresponding indices, $1 \le l \le 3N_p$ and $6N_p + N_1 < l \le 6N_p + N_1 + N_2$, respectively. Considering the terms $\mathcal{J}_{lk}(\mathbf{u})$, $\mathcal{J}_{li}(\mathbf{u})$ and $\mathcal{J}_{lj}(\mathbf{u})$, we see that in these index ranges, only

$J_{12} = \mathbb{M}_p^{-1}$ and $J_{43} = -M_2^{-1}\mathbb{C}M_1^{-1}$ are non-vanishing, so that we have to account only for those two blocks. Note that J_{12} is a diagonal matrix, therefore $(J_{12})_{ij} = (J_{12})_{ii}\delta_{ij}$. Further, only J_{22}, J_{23} and J_{32} depend on $\mathbf{b}$ and/or $\mathbf{X}$, so only those blocks have to be considered when computing derivatives with respect to $\mathbf{u}$. In summary, we have

$$\mathcal{J}(\mathbf{u}) = \begin{pmatrix} 0 & J_{12} & 0 & 0 \\ J_{21} & J_{22}(\mathbf{X}, \mathbf{b}) & J_{23}(\mathbf{X}) & 0 \\ 0 & J_{32}(\mathbf{X}) & 0 & J_{34} \\ 0 & 0 & J_{43} & 0 \end{pmatrix}, \tag{83}$$

and obtain two conditions. From the contributions involving J_{22} and J_{12} we have

$$\sum_{l=1}^{3N_p} \left(\frac{\partial\big(J_{22}(\mathbf{X}, \mathbf{b})\big)_{ij}}{\partial\mathbf{X}_l}\,(J_{12})_{lk} + \frac{\partial\big(J_{22}(\mathbf{X}, \mathbf{b})\big)_{jk}}{\partial\mathbf{X}_l}\,(J_{12})_{li} + \frac{\partial\big(J_{22}(\mathbf{X}, \mathbf{b})\big)_{ki}}{\partial\mathbf{X}_l}\,(J_{12})_{lj} \right) = 0, \tag{84}$$

for $1 \le i, j, k \le 3N_p$, which corresponds to (81) for $3N_p < i, j, k \le 6N_p$. Inserting the actual values for J_{12} and J_{22} and using that M_p is diagonal, (84) becomes

$$\frac{\partial\big(\mathbb{M}_p^{-1}\mathbb{M}_q\mathbb{B}(\mathbf{X}, \mathbf{b})\,\mathbb{M}_p^{-1}\big)_{ij}}{\partial\mathbf{X}_k}\,\big(\mathbb{M}_p^{-1}\big)_{kk} + \frac{\partial\big(\mathbb{M}_p^{-1}\mathbb{M}_q\mathbb{B}(\mathbf{X}, \mathbf{b})\,\mathbb{M}_p^{-1}\big)_{jk}}{\partial\mathbf{X}_i}\,\big(\mathbb{M}_p^{-1}\big)_{ii}$$
$$+ \frac{\partial\big(\mathbb{M}_p^{-1}\mathbb{M}_q\mathbb{B}(\mathbf{X}, \mathbf{b})\,\mathbb{M}_p^{-1}\big)_{ki}}{\partial\mathbf{X}_j}\,\big(\mathbb{M}_p^{-1}\big)_{jj} = 0. \tag{85}$$

All outer indices of this expression belong to the inverse matrix M_p^{-1}. As this matrix is constant, symmetric and positive definite, we can contract the above expression with M_p on all indices, to obtain

$$\frac{\partial\big(\mathbb{M}_q\mathbb{B}(\mathbf{X}, \mathbf{b})\big)_{ij}}{\partial\mathbf{X}_k} + \frac{\partial\big(\mathbb{M}_q\mathbb{B}(\mathbf{X}, \mathbf{b})\big)_{jk}}{\partial\mathbf{X}_i} + \frac{\partial\big(\mathbb{M}_q\mathbb{B}(\mathbf{X}, \mathbf{b})\big)_{ki}}{\partial\mathbf{X}_j} = 0, \qquad 1 \le i, j, k \le 3N_p. \tag{86}$$

Consider the first term of this expression. Picking one particular index k, selects the σ component of the position $\mathbf{x}_a$ of some particle. At the same time, in the second and third term, this selects a block of (75), which is evaluated at the same particle position $\mathbf{x}_a$. This means that the only non-vanishing contributions in (86) will be for i and j for which $\mathbf{X}_i$ and $\mathbf{X}_j$ correspond to components μ and ν of the same particle position $\mathbf{x}_a$. Therefore, the condition (75) reduces further to

$$q_a \left(\frac{\partial\widehat{B}_{\mu\nu}(\mathbf{x}_a)}{\partial\mathrm{x}_a^\sigma} + \frac{\partial\widehat{B}_{\nu\sigma}(\mathbf{x}_a)}{\partial\mathrm{x}_a^\mu} + \frac{\partial\widehat{B}_{\sigma\mu}(\mathbf{x}_a)}{\partial\mathrm{x}_a^\nu} \right) = 0, \qquad 1 \le a \le N_p, \quad 1 \le \mu, \nu, \sigma \le 3, \tag{87}$$

where $\widehat{B}_{\mu\nu}$ denotes the components of the matrix in (75). When all three indices are equal, this corresponds to diagonal terms of the matrix $\widehat{\mathbf{B}}_h(\mathbf{x}_a, t)$ which vanish. When two of the three are equal, it cancels because of the skew-symmetry of the same matrix and for all three indices distinct, this condition corresponds to $\operatorname{div}\mathbf{B}_h = 0$. Choosing initial conditions such that $\operatorname{div}\mathbf{B}_h(\mathbf{x}, 0) = 0$ and using a discrete deRham complex guarantees $\operatorname{div}\mathbf{B}_h(\mathbf{x}, t) = 0$ for all times t.

From the contributions involving J_{22}, J_{23}, J_{32} and J_{43} we have

$$\sum_{l=1}^{3N_p} \left(\frac{\partial\big(J_{23}(\mathbf{X}, \mathbf{b})\big)_{jk}}{\partial \mathbf{X}_l} \big(J_{12}\big)_{li} + \frac{\partial\big(J_{32}(\mathbf{X}, \mathbf{b})\big)_{ki}}{\partial \mathbf{X}_l} \big(J_{12}\big)_{lj} \right)$$
$$+ \sum_{l=1}^{N_2} \frac{\partial\big(J_{22}(\mathbf{X}, \mathbf{b})\big)_{ij}}{\partial \mathbf{b}_l} \big(J_{43}\big)_{lk} = 0, \quad (88)$$

for $1 \le i,j \le 3N_p$ and $1 \le k \le N_1$, which corresponds to (81) for $3N_p < i,j \le 6N_p < k \le 6N_p + N_1$. Writing out (88) and using that M_p is diagonal, we have

$$\frac{\partial\big(M_1^{-1}\mathbb{A}^1(\mathbf{X})^\top \mathbb{M}_q \mathbb{M}_p^{-1}\big)_{ki}}{\partial \mathbf{X}_j} \big(\mathbb{M}_p^{-1}\big)_{jj} - \frac{\partial\big(\mathbb{M}_p^{-1}\mathbb{M}_q\mathbb{A}^1(\mathbf{X}) M_1^{-1}\big)_{jk}}{\partial \mathbf{X}_i} \big(\mathbb{M}_p^{-1}\big)_{ii} =$$
$$= \sum_{l=1}^{N_2} \frac{\partial\big(\mathbb{M}_p^{-1}\mathbb{M}_q\mathbb{B}(\mathbf{X}, \mathbf{b})\, \mathbb{M}_p^{-1}\big)_{ij}}{\partial \mathbf{b}_l} \big(\mathbb{C} M_1^{-1}\big)_{lk}. \quad (89)$$

Again, we can contract this with the matrix M_p on the indices i and j, in order to remove M_p^{-1}, as well as with M_1 on the index k, in order to remove M_1^{-1}. This results in the simplified condition

$$\frac{\partial\big(\mathbb{A}^1(\mathbf{X})^\top \mathbb{M}_q\big)_{ki}}{\partial \mathbf{X}_j} - \frac{\partial\big(\mathbb{M}_q\mathbb{A}^1(\mathbf{X})\big)_{jk}}{\partial \mathbf{X}_i} = \sum_{l=1}^{N_2} \frac{\partial\big(\mathbb{M}_q\mathbb{B}(\mathbf{X}, \mathbf{b})\big)_{ij}}{\partial \mathbf{b}_l} \big(\mathbb{C}\big)_{lk}. \quad (90)$$

The $\mathbf{b}_l$ derivative of $\mathbb{B}$ results in the $3N_p \times 3N_p$ block diagonal matrix $\mathbb{A}_l^2(\mathbf{X})$ with generic block

$$\widehat{\mathbf{\Lambda}}_l^2(\mathbf{x}_a) = \begin{pmatrix} 0 & \Lambda_l^{2,3}(\mathbf{x}_a) & -\Lambda_l^{2,2}(\mathbf{x}_a) \\ -\Lambda_l^{2,3}(\mathbf{x}_a) & 0 & \Lambda_l^{2,1}(\mathbf{x}_a) \\ \Lambda_l^{2,2}(\mathbf{x}_a) & -\Lambda_l^{2,1}(\mathbf{x}_a) & 0 \end{pmatrix}, \quad (91)$$

so that (90) becomes

$$\frac{\partial\big(\mathbb{A}^1(\mathbf{X})^\top \mathbb{M}_q\big)_{ki}}{\partial \mathbf{X}_j} - \frac{\partial\big(\mathbb{M}_q\mathbb{A}^1(\mathbf{X})\big)_{jk}}{\partial \mathbf{X}_i} = \sum_{l=1}^{N_2} \big(\mathbb{M}_q\mathbb{A}_l^2(\mathbf{X})\big)_{ij} \big(\mathbb{C}\big)_{lk}. \quad (92)$$

Similarly as before, considering the first term, picking one particular index j, selects the ν component of the position $\mathbf{x}_a$ of some particle. At the same time, in the second term, this selects the ν component of $\mathbf{\Lambda}^1$, evaluated at the same particle position $\mathbf{x}_a$. The only non-vanishing derivative of this term is therefore with respect to components of the same particle position, so that $\mathbf{X}_i$ denotes the μ component of $\mathbf{x}_a$. Hence, condition (92) simplifies to

$$q_a \left(\frac{\partial \mathbf{\Lambda}_k^{1,\mu}(\mathbf{x}_a)}{\partial \mathrm{x}_a^\nu} - \frac{\partial \mathbf{\Lambda}_k^{1,\nu}(\mathbf{x}_a)}{\partial \mathrm{x}_a^\mu} \right) = q_a \sum_{l=1}^{N_2} \big(\widehat{\mathbf{\Lambda}}_l^2(\mathbf{x}_a)\big)_{\mu\nu} \big(\mathbb{C}\big)_{lk}, \quad (93)$$

for $1 \le a \le N_p$, $1 \le \mu,\nu \le 3$ and $1 \le k \le N_1$. This conditions states that the curl of the one-form basis, evaluated at some particle's position, equals the two-form basis, evaluated at the same particle's position.

19

4.5 Discrete Hamiltonian and Equations of Motion

The Hamiltonian is discretized by inserting (70) and (48) into (11),

$$
\mathcal{H}_h = \frac{1}{2} \int |\mathbf{v}|^2 \sum_{a=1}^{N_p} m_a w_a\, \delta\big(\mathbf{x} - \mathbf{x}_a(t)\big)\, \delta\big(\mathbf{v} - \mathbf{v}_a(t)\big)\, \mathrm{d}\mathbf{x}\, \mathrm{d}\mathbf{v}
$$

$$
+ \frac{1}{2} \int \left| \sum_{i=1}^{N_1} e_i(t)\, \boldsymbol{\Lambda}_i^1(\mathbf{x}) \right|^2 \mathrm{d}\mathbf{x} + \frac{1}{2} \int \left| \sum_{j=1}^{N_2} b_j(t)\, \boldsymbol{\Lambda}_j^2(\mathbf{x}) \right|^2 \mathrm{d}\mathbf{x} \tag{94}
$$

which in matrix notation becomes

$$
\hat{\mathcal{H}} = \tfrac{1}{2}\, \mathbf{V}^\top \mathbb{M}_p \mathbf{V} + \tfrac{1}{2}\, \mathbf{e}^\top M_1 \mathbf{e} + \tfrac{1}{2}\, \mathbf{b}^\top M_2 \mathbf{b}. \tag{95}
$$

In order to compute the semi-discrete equations of motion, we consider

$$
\dot{\mathbf{X}} = \{\mathbf{X}, \hat{\mathcal{H}}\}, \qquad \dot{\mathbf{V}} = \{\mathbf{V}, \hat{\mathcal{H}}\}, \qquad \dot{\mathbf{e}} = \{\mathbf{e}, \hat{\mathcal{H}}\}, \qquad \dot{\mathbf{b}} = \{\mathbf{b}, \hat{\mathcal{H}}\}, \tag{96}
$$

which is equivalent to

$$
\dot{\mathbf{u}} = \mathcal{J}(\mathbf{u})\, \mathrm{D}\mathcal{H}(\mathbf{u}). \tag{97}
$$

With $\mathrm{D}\mathcal{H}(\mathbf{u}) = (0,\, \mathbb{M}_p \mathbf{V},\, M_1 \mathbf{e},\, M_2 \mathbf{b})^\top$, we obtain

$$
\dot{\mathbf{X}} = \mathbf{V}, \tag{98a}
$$

$$
\dot{\mathbf{V}} = \mathbb{M}_p^{-1} \mathbb{M}_q \big(\mathbb{A}^1(\mathbf{X})\mathbf{e} + \mathbb{B}(\mathbf{X}, \mathbf{b})\mathbf{V} \big), \tag{98b}
$$

$$
\dot{\mathbf{e}} = M_1^{-1} \big(\mathbb{C}^\top M_2 \mathbf{b}(t) - \mathbb{A}^1(\mathbf{X})^\top \mathbb{M}_q \mathbf{V} \big), \tag{98c}
$$

$$
\dot{\mathbf{b}} = -\mathbb{C}\mathbf{e}(t), \tag{98d}
$$

where the first two equations describe the particle dynamics and the last two equations the evolution of the electromagnetic fields.

4.6 Discrete Gauss' Law

Multiplying (98c) by $\mathbb{G}^\top M_1$ on the left, we get

$$
\mathbb{G}^\top M_1 \dot{\mathbf{e}} = \mathbb{G}^\top \mathbb{C}^\top M_2 \mathbf{b}(t) - \mathbb{G}^\top \mathbb{A}^1(\mathbf{X})^\top \mathbb{M}_q \mathbf{V}. \tag{99}
$$

As $\mathbb{C}\mathbb{G} = 0$ from (56), the first term on the right-hand side vanishes. Observe that

$$
\mathbb{A}^1(\mathbf{X})\mathbb{G}\psi = \nabla \mathbb{A}^0(\mathbf{X})\psi \quad \forall \psi \in \mathbb{R}^{N_0}, \tag{100}
$$

as well as that using $\frac{\mathrm{d}\mathbf{x}_a}{\mathrm{d}t} = \mathbf{v}_a$, we find that

$$
\frac{\mathrm{d}\Psi_h(\mathbf{x}_a(t))}{\mathrm{d}t} = \frac{\mathrm{d}\mathbf{x}_a(t)}{\mathrm{d}t} \cdot \nabla \Psi_h(\mathbf{x}_a(t)) = \mathbf{v}_a \cdot \nabla \Psi_h(\mathbf{x}_a(t)), \tag{101}
$$

for any $\Psi_h \in V_0$ with $\nabla \Psi_h \in V_1$, so that we get

$$
\mathbb{G}^\top M_1 \dot{\mathbf{e}} = -\mathbb{G}^\top \mathbb{A}^1(\mathbf{X})^\top \mathbb{M}_q \mathbf{V} = -\nabla \mathbb{A}^0(\mathbf{X})^\top \mathbb{M}_q \mathbf{V} = -\frac{\mathrm{d}\mathbb{A}^0(\mathbf{X})^\top}{\mathrm{d}t} \mathbb{M}_q \mathbb{1}_{N_p}, \tag{102}
$$

where $\mathbb{1}_{N_p}$ denotes the column vector with N_p terms all being one, needed for the sum over the particles, when there is no velocity vector. This shows that the discrete Gauss' law is conserved,

$$
\mathbb{G}^\top M_1 \mathbf{e} = -\mathbb{A}^0(\mathbf{X})^\top \mathbb{M}_q \mathbb{1}_{N_p}. \tag{103}
$$

4.7 Casimirs

Let us now find the Casimirs of the semi-discrete Poisson structure. These are functionals $\mathcal{C}(\mathbf{X}, \mathbf{V}, \mathbf{e}, \mathbf{b})$ such that $\{\mathcal{C}, \mathcal{F}\}$ for any function $\mathcal{F}$. In terms of the Poisson matrix $\mathcal{J}$, this can be expressed as $\mathcal{J}(\mathbf{u}) D\mathcal{C}(\mathbf{u}) = 0$. Decomposing this line by line of the block matrix, we find for the first line

$$M_m^{-1} D_{\mathbf{V}} \mathcal{C} = 0.$$

This implies that $\mathcal{C}$ does not depend on $\mathbf{V}$, which we shall use in the sequel. Then the third line simply becomes

$$M_1^{-1} \mathbb{C}^\top D_{\mathbf{b}} \mathcal{C} = 0 \Rightarrow D_{\mathbf{b}} \mathcal{C} \in \mathrm{Ker}(\mathbb{C}^\top).$$

Then, because of the exact sequence property, there exists $\tilde{\mathbf{b}} \in \mathbb{R}^{N_3}$ such that $D_{\mathbf{b}} \mathcal{C} = \mathbb{D}^\top \tilde{\mathbf{b}}$. Hence all functions of the form

$$\mathcal{C}(\mathbf{b}) = \mathbf{b}^\top \mathbb{D}^\top \tilde{\mathbf{b}} = \tilde{\mathbf{b}}^\top \mathbb{D}\mathbf{b}, \quad \tilde{\mathbf{b}} \in \mathbb{R}^{N_3} \tag{104}$$

are Casimirs, which means that $\mathbb{D}\mathbf{b}$, the matrix form of $\mathrm{div}\,\mathbf{B}_h$, is conserved.

The fourth line, using that $\mathcal{C}$ does not depend on $\mathbf{V}$, becomes

$$\mathbb{C} M_1^{-1} D_{\mathbf{e}} \mathcal{C} = 0 \Rightarrow M_1^{-1} D_{\mathbf{e}} \mathcal{C} \in \mathrm{Ker}(\mathbb{C}),$$

so because of the exact sequence property there exists $\tilde{\mathbf{e}} \in \mathbb{R}^{N_1}$ such that $D_{\mathbf{e}} \mathcal{C} = M_1 \mathbb{G} \tilde{\mathbf{e}}$. Finally the second line couples $\mathbf{e}$ and $\mathbf{X}$ and reads, multiplying by M_p

$$D_{\mathbf{X}} \mathcal{C} = M_q \mathbb{A}^1(\mathbf{X}) M_1^{-1} D_{\mathbf{e}} \mathcal{C} = M_q \mathbb{A}^1(\mathbf{X}) \mathbb{G} \tilde{\mathbf{e}} = M_q \nabla \mathbb{A}_0(\mathbf{X}) \tilde{\mathbf{e}},$$

using the expression of $D_{\mathbf{e}} \mathcal{C}$ derived previously and (100). So it follows that all functions of the form

$$\mathcal{C}(\mathbf{X}, \mathbf{e}) = \mathbb{1}_N^\top M_q \mathbb{A}^0(\mathbf{X}) \tilde{\mathbf{e}} + \mathbf{e}^\top M_1 \mathbb{G} \tilde{\mathbf{e}} = \tilde{\mathbf{e}}^\top \mathbb{A}^0(\mathbf{X})^\top M_q \mathbb{1}_N + \tilde{\mathbf{e}}^\top \mathbb{G}^\top M_1 \mathbf{e}, \quad \tilde{\mathbf{e}} \in \mathbb{R}^{N_0} \tag{105}$$

are Casimirs, which means that $\mathbb{G}^\top M_1 \mathbf{e} + \mathbb{A}^0(\mathbf{X})^\top M_q \mathbb{1}_N$ is conserved. This is the matrix form of Gauss' law (103).

5 Hamiltonian Splitting

Following [29, 66, 40], we split the discrete Hamiltonian (95) into three parts,

$$\hat{\mathcal{H}} = \hat{\mathcal{H}}_p + \hat{\mathcal{H}}_E + \hat{\mathcal{H}}_B, \tag{106}$$

with

$$\hat{\mathcal{H}}_p = \tfrac{1}{2} \mathbf{V}^\top \mathbb{M}_p \mathbf{V}, \qquad \hat{\mathcal{H}}_E = \tfrac{1}{2} \mathbf{e}^\top M_1 \mathbf{e}, \qquad \hat{\mathcal{H}}_B = \tfrac{1}{2} \mathbf{b}^\top M_2 \mathbf{b}. \tag{107}$$

Writing $\mathbf{u} = (\mathbf{X}, \mathbf{V}, \mathbf{e}, \mathbf{b})$, we split the discrete Vlasov-Maxwell equations (98a)-(98d) into three subsystems,

$$\dot{\mathbf{u}} = \{\mathbf{u}, \hat{\mathcal{H}}_p\}, \qquad \dot{\mathbf{u}} = \{\mathbf{u}, \hat{\mathcal{H}}_E\}, \qquad \dot{\mathbf{u}} = \{\mathbf{u}, \hat{\mathcal{H}}_B\}. \tag{108}$$

The exact solution to each of these subsystems will constitute a Poisson map. Because a composition of Poisson maps is itself a Poisson map, we can construct Poisson structure preserving integration methods for the Vlasov-Maxwell system by composition of the exact solutions.

5.1 Solution of the Sub-Systems

The discrete equations of motion for $\hat{\mathcal{H}}_E$ are

$$\dot{\mathbf{X}} = 0, \tag{109a}$$

$$\mathbb{M}_p \dot{\mathbf{V}} = \mathbb{M}_q \mathbb{A}^1(\mathbf{X}) \mathbf{e}, \tag{109b}$$

$$\dot{\mathbf{e}} = 0, \tag{109c}$$

$$\dot{\mathbf{b}} = -\mathbb{C} \mathbf{e}(t). \tag{109d}$$

For initial conditions $\big(\mathbf{X}(0), \mathbf{V}(0), \mathbf{e}(0), \mathbf{b}(0)\big)$ the exact solutions at time Δt are given by

$$\mathbf{X}(\Delta t) = \mathbf{X}(0), \tag{110a}$$

$$\mathbb{M}_p \mathbf{V}(\Delta t) = \mathbb{M}_p \mathbf{V}(0) + \Delta t \, \mathbb{M}_q \mathbb{A}^1(\mathbf{X}(0)) \mathbf{e}(0), \tag{110b}$$

$$\mathbf{e}(\Delta t) = \mathbf{e}(0), \tag{110c}$$

$$\mathbf{b}(\Delta t) = \mathbf{b}(0) - \Delta t \, \mathbb{C} \mathbf{e}(0). \tag{110d}$$

The discrete equations of motion for $\hat{\mathcal{H}}_B$ are

$$\dot{\mathbf{X}} = 0, \tag{111a}$$

$$\dot{\mathbf{V}} = 0, \tag{111b}$$

$$M_1 \dot{\mathbf{e}} = \mathbb{C}^\top M_2 \mathbf{b}(t), \tag{111c}$$

$$\dot{\mathbf{b}} = 0. \tag{111d}$$

For initial conditions $\big(\mathbf{X}(0), \mathbf{V}(0), \mathbf{e}(0), \mathbf{b}(0)\big)$ the exact solutions at time Δt are given by

$$\mathbf{X}(\Delta t) = \mathbf{X}(0), \tag{112a}$$

$$\mathbf{V}(\Delta t) = \mathbf{V}(0), \tag{112b}$$

$$M_1 \mathbf{e}(\Delta t) = M_1 \mathbf{e}(0) + \Delta t \, \mathbb{C}^\top M_2 \mathbf{b}(0), \tag{112c}$$

$$\mathbf{b}(\Delta t) = \mathbf{b}(0). \tag{112d}$$

The discrete equations of motion for $\hat{\mathcal{H}}_p$ are

$$\dot{\mathbf{X}} = \mathbf{V}, \tag{113a}$$

$$\mathbb{M}_p \dot{\mathbf{V}} = \mathbb{M}_q \mathbb{B}(\mathbf{X}, \mathbf{b}) \mathbf{V}, \tag{113b}$$

$$M_1 \dot{\mathbf{e}} = -\mathbb{A}^1(\mathbf{X})^\top \mathbb{M}_q \mathbf{V}, \tag{113c}$$

$$\dot{\mathbf{b}} = 0, \tag{113d}$$

For general magnetic field coefficients $\mathbf{b}$, this system cannot be exactly integrated [40]. Note that each component $\dot{\mathbf{V}}^\mu$ of the equation for $\dot{\mathbf{V}}$ does not depend on $\mathbf{V}^\mu$, where $\mathbf{V}^\mu = (v_1^\mu, v_2^\mu, \ldots, v_{N_p}^\mu)^\top$, etc., with $1 \leq \mu \leq 3$. Therefore we can split this system once more into

$$\hat{\mathcal{H}}_p = \hat{\mathcal{H}}_{p_1} + \hat{\mathcal{H}}_{p_2} + \hat{\mathcal{H}}_{p_3}, \tag{114}$$

with

$$\hat{\mathcal{H}}_{p_\mu} = \tfrac{1}{2} (\mathbf{V}^\mu)^\top M_p \mathbf{V}^\mu \qquad \text{for} \qquad 1 \leq \mu \leq 3. \tag{115}$$

For concise notation we introduce the $N_p \times N_1$ matrix $\mathbb{A}^{1,\mu}(\mathbf{X})$ with generic term $\Lambda_i^{1,\mu}(\mathbf{x}_a)$, and the $N_p \times N_p$ diagonal matrix $\mathbb{A}^{2,\mu}(\mathbf{b}, \mathbf{X})$ with entries $\sum_{i=1}^{N_2} b_i(t)\Lambda_i^{2,\mu}(\mathbf{x}_a)$, where $1 \leq \mu \leq 3$, $1 \leq a \leq N_p$, $1 \leq i \leq N_1$, $1 \leq j \leq N_2$. Then, for $\hat{\mathcal{H}}_{p_1}$ we have

$$\dot{\mathbf{X}}^1 = \mathbf{V}^1(t), \tag{116a}$$

$$M_p\dot{\mathbf{V}}^2 = -M_q\mathbb{A}^{2,3}(\mathbf{b}(t), \mathbf{X}(t))^\top \mathbf{V}^1(t), \tag{116b}$$

$$M_p\dot{\mathbf{V}}^3 = M_q\mathbb{A}^{2,2}(\mathbf{b}(t), \mathbf{X}(t))^\top \mathbf{V}^1(t), \tag{116c}$$

$$M_1\dot{\mathbf{e}} = -\mathbb{A}^{1,1}(\mathbf{X}(t))^\top M_q\mathbf{V}^1(t), \tag{116d}$$

for $\hat{\mathcal{H}}_{p_2}$ we have

$$\dot{\mathbf{X}}^2 = \mathbf{V}^2(t), \tag{117a}$$

$$M_p\dot{\mathbf{V}}^1 = M_q\mathbb{A}^{2,3}(\mathbf{b}(t), \mathbf{X}(t))^\top \mathbf{V}^2(t), \tag{117b}$$

$$M_p\dot{\mathbf{V}}^3 = -M_q\mathbb{A}^{2,1}(\mathbf{b}(t), \mathbf{X}(t))^\top \mathbf{V}^2(t), \tag{117c}$$

$$M_1\dot{\mathbf{e}} = -\mathbb{A}^{1,2}(\mathbf{X}(t))^\top M_q\mathbf{V}^2(t), \tag{117d}$$

and for $\hat{\mathcal{H}}_{p_3}$ we have

$$\dot{\mathbf{X}}^3 = \mathbf{V}^3(t), \tag{118a}$$

$$M_p\dot{\mathbf{V}}^1 = -M_q\mathbb{A}^{2,2}(\mathbf{b}(t), \mathbf{X}(t))^\top \mathbf{V}^3(t), \tag{118b}$$

$$M_p\dot{\mathbf{V}}^2 = M_q\mathbb{A}^{2,1}(\mathbf{b}(t), \mathbf{X}(t))^\top \mathbf{V}^3(t), \tag{118c}$$

$$M_1\dot{\mathbf{e}} = -\mathbb{A}^{1,3}(\mathbf{X}(t))^\top M_q\mathbf{V}^3(t), \tag{118d}$$

For initial conditions $\big(\mathbf{X}(0), \mathbf{V}(0), \mathbf{e}(0), \mathbf{b}(0)\big)$ the exact solutions at time Δt are given by

$$\mathbf{X}^1(\Delta t) = \mathbf{X}^1(0) + \Delta t\, \mathbf{V}^1(0), \tag{119a}$$

$$M_p\mathbf{V}^2(\Delta t) = M_p\mathbf{V}^2(0) + \int_0^{\Delta t} M_q\mathbb{A}^{2,3}(\mathbf{b}(0), \mathbf{X}(t))\, \mathbf{V}^1(0)\, \mathrm{d}t, \tag{119b}$$

$$M_p\mathbf{V}^3(\Delta t) = M_p\mathbf{V}^3(0) - \int_0^{\Delta t} M_q\mathbb{A}^{2,2}(\mathbf{b}(0), \mathbf{X}(t))\, \mathbf{V}^1(0)\, \mathrm{d}t, \tag{119c}$$

$$M_1\mathbf{e}(\Delta t) = M_1\mathbf{e}(0) - \int_0^{\Delta t} \mathbb{A}^{1,1}(\mathbf{X}(t))^\top M_q\mathbf{V}_p^1(0)\, \mathrm{d}t, \tag{119d}$$

for $\hat{\mathcal{H}}_{p_1}$, by

$$\mathbf{X}^2(\Delta t) = \mathbf{X}^2(0) + \Delta t\, \mathbf{V}^2(0), \tag{120a}$$

$$M_p\mathbf{V}^1(\Delta t) = M_p\mathbf{V}^1(0) - \int_0^{\Delta t} M_q\mathbb{A}^{2,3}(\mathbf{b}(0), \mathbf{X}(t))\, \mathbf{V}^2(0)\, \mathrm{d}t, \tag{120b}$$

$$M_p\mathbf{V}^3(\Delta t) = M_p\mathbf{V}^3(0) + \int_0^{\Delta t} M_q\mathbb{A}^{2,1}(\mathbf{b}(0), \mathbf{X}(t))\, \mathbf{V}^2(0)\, \mathrm{d}t, \tag{120c}$$

$$M_1\mathbf{e}(\Delta t) = M_1\mathbf{e}(0) - \int_0^{\Delta t} \mathbb{A}^{1,2}(\mathbf{X}(t))^\top M_q\mathbf{V}^2(0)\, \mathrm{d}t, \tag{120d}$$

23

for $\hat{\mathcal{H}}_{p_2}$, and by

$$\mathbf{X}^3(\Delta t) = \mathbf{X}^3(0) + \Delta t\, \mathbf{V}^3(0), \tag{121a}$$

$$M_p\mathbf{V}^1(\Delta t) = M_p\mathbf{V}^1(0) + \int_0^{\Delta t} M_q \mathbb{A}^{2,2}(\mathbf{b}(0), \mathbf{X}(t))\, \mathbf{V}^3(0)\, \mathrm{d}t, \tag{121b}$$

$$M_p\mathbf{V}^2(\Delta t) = M_p\mathbf{V}^2(0) - \int_0^{\Delta t} M_q \mathbb{A}^{2,1}(\mathbf{b}(0), \mathbf{X}(t))\, \mathbf{V}^3(0)\, \mathrm{d}t, \tag{121c}$$

$$M_1\mathbf{e}(\Delta t) = M_1\mathbf{e}(0) - \int_0^{\Delta t} \mathbb{A}^{1,3}(\mathbf{X}(t))^\top M_q\mathbf{V}^3(0)\, \mathrm{d}t, \tag{121d}$$

for $\hat{\mathcal{H}}_{p_3}$, respectively, where all components not specified are constant. The only challenge in solving these equations is the exact computation of line integrals along the trajectories [18, 71, 54]. However, as only one component of the particle positions x_p is changing in each step of the splitting, and moreover the trajectory is given by a straight line, this is not very complicated.

5.2 Splitting Methods

Given initial conditions $\mathbf{u}(0) = \big(\mathbf{X}(0), \mathbf{V}(0), \mathbf{e}(0), \mathbf{b}(0)\big)$, a numerical solution of the discrete Vlasov-Maxwell equations (98a)-(98d) at time h can be obtained by composition of the exact solutions of all the subsystems. A first order integrator can be obtained by the Lie-Trotter composition

$$\mathbf{u}(\Delta t) = \exp(\Delta t\, X_E)\exp(\Delta t\, X_B)\exp(\Delta t\, X_{p_1})\exp(\Delta t\, X_{p_2})\exp(\Delta t\, X_{p_3})\,\mathbf{u}(0), \tag{122}$$

where X_E, etc., denote the Hamiltonian vector fields corresponding to $\hat{\mathcal{H}}_E$, etc., that is e.g. $X_E = \mathcal{J}(\cdot, \mathrm{D}\hat{\mathcal{H}}_E)$. A second order integrator can be obtain by the symmetric Strang composition

$$\begin{aligned}\mathbf{u}(\Delta t) =\ & \exp(\Delta t/2\, X_E)\exp(\Delta t/2\, X_B)\exp(\Delta t/2\, X_{p_1})\exp(\Delta t/2\, X_{p_2})\exp(\Delta t/2\, X_{p_3})\\ & \exp(\Delta t/2\, X_{p_3})\exp(\Delta t/2\, X_{p_2})\exp(\Delta t/2\, X_{p_1})\exp(\Delta t/2\, X_B)\exp(\Delta t/2\, X_E)\,\mathbf{u}(0).\end{aligned} \tag{123}$$

The corresponding maps can be written as

$$\varphi_{\Delta t, L} = \varphi_{\Delta t, p_3} \circ \varphi_{\Delta t, p_2} \circ \varphi_{\Delta t, p_1} \circ \varphi_{\Delta t, B} \circ \varphi_{\Delta t, E}, \tag{124}$$

and

$$\varphi_{\Delta t, S2} = \varphi_{\Delta t/2, L} \circ \varphi^*_{\Delta t/2, L}, \tag{125}$$

respectively, where $\varphi^*_{\Delta t, L}$ denotes the adjoint of $\varphi_{\Delta t, L}$, that is

$$\varphi^*_{\Delta t, L} = \varphi^{-1}_{-\Delta t, L}. \tag{126}$$

Let us note that the Lie splitting $\varphi_{\Delta t, L}$ and the Strang splitting $\varphi_{\Delta t, S2}$ are conjugate methods by the adjoint of $\varphi_{\Delta t, L}$, i.e.,

$$\varphi_{\Delta t, S2} = \big(\varphi^*_{\Delta t/2, L}\big)^{-1} \circ \varphi_{\Delta t, L} \circ \varphi^*_{\Delta t/2, L} = \varphi_{-\Delta t/2, L} \circ \varphi_{\Delta t, L} \circ \varphi^*_{\Delta t/2, L} = \varphi_{\Delta t/2, L} \circ \varphi^*_{\Delta t/2, L}. \tag{127}$$

The last equality holds by the group property of the flow, but is only valid when the exact solution of each subsystem is used in the composition (and not some general symplectic integrator). This implies that the Lie splitting shares many properties with the Strang splitting which are not found in general first order methods.

Another second order integrator with smaller error constant than $\varphi_{\Delta t, S2}$ can be obtained by the following composition,

$$\varphi_{\Delta t, L2} = \varphi_{\alpha \Delta t, L} \circ \varphi^*_{(1/2-\alpha)\Delta t, L} \circ \varphi_{(1/2-\alpha)\Delta t, L} \circ \varphi^*_{\alpha \Delta t, L}. \tag{128}$$

Here, α is a free parameter which can be used to reduce the error constant. A particular small error is obtained for $\alpha = 0.1932$. Fourth order time integrators can easily be obtained from a second order integrator like $\varphi_{\Delta t, S}$ by the following composition,

$$\varphi_{\Delta t, S4} = \varphi_{\gamma_1 \Delta t, S2} \circ \varphi_{\gamma_2 \Delta t, S2} \circ \varphi_{\gamma_1 \Delta t, S2}, \tag{129}$$

with

$$\gamma_1 = \frac{1}{2 - 2^{1/3}}, \qquad\qquad \gamma_2 = -\frac{2^{1/3}}{2 - 2^{1/3}}.$$

Alternatively, we can compose the first order integrator $\varphi_{\Delta t, L}$ together with its adjoint $\varphi^*_{\Delta t, L}$ as follows,

$$\varphi_{\Delta t, L4} = \varphi_{a_5 \Delta t, L} \circ \varphi^*_{b_5 \Delta t, L} \circ \cdots \circ \varphi_{a_2 \Delta t, L} \circ \varphi^*_{b_2 \Delta t, L} \circ \varphi_{a_1 \Delta t, L} \circ \varphi^*_{b_1 \Delta t, L}, \tag{130}$$

with

$$a_1 = b_5 = \frac{146 + 5\sqrt{19}}{540}, \qquad a_2 = b_4 = \frac{-2 + 10\sqrt{19}}{135}, \qquad a_3 = b_3 = \frac{1}{5},$$

$$a_4 = b_2 = \frac{-23 - 20\sqrt{19}}{270}, \qquad a_5 = b_1 = \frac{14 - \sqrt{19}}{108}.$$

For higher order composition methods see e.g. [39] and [52] and references therein.

5.3 Backward Error Analysis

In the following, we want to compute the modified Hamiltonians for the Lie-Trotter splitting as well as the Strang splitting. Following Hairer et al. [39, Chapter IX], the modified Hamiltonian of the Lie-Trotter splitting

$$\varphi_{\Delta t} = \varphi_{\Delta t, B} \circ \varphi_{\Delta t, A}, \tag{131}$$

where $\mathcal{H} = \mathcal{H}_A + \mathcal{H}_B$, is given by

$$\tilde{\mathcal{H}} = \mathcal{H} + \Delta t \tilde{\mathcal{H}}_1 + \Delta t^2 \tilde{\mathcal{H}}_2 + \mathcal{O}(\Delta t^3), \tag{132}$$

with

$$\tilde{\mathcal{H}}_1 = \frac{1}{2}\{\mathcal{H}_A, \mathcal{H}_B\}, \tag{133}$$

$$\tilde{\mathcal{H}}_2 = \frac{1}{12}\big[\{\{\mathcal{H}_A, \mathcal{H}_B\}, \mathcal{H}_B\} + \{\{\mathcal{H}_B, \mathcal{H}_A\}, \mathcal{H}_A\}\big]. \tag{134}$$

In order to compute the modified Hamiltonian for splittings with more than two terms, we have to apply the Baker–Campbell–Hausdorff formula recursively.

25

Lie-Trotter Splitting For the Lie-Trotter splitting (124), expressed in terms of the corresponding Hamiltonian vector fields as

$$\varphi_{\Delta t} = \exp(\Delta t\, X_E)\exp(\Delta t\, X_B)\exp(\Delta t\, X_{p_1})\exp(\Delta t\, X_{p_2})\exp(\Delta t\, X_{p_3}) = \exp(\Delta t\, \tilde{X}), \tag{135}$$

we split φ_h into

$$\exp(\Delta t\, X_E)\exp(\Delta t\, X_B) = \exp(\Delta t\, \tilde{X}_{EB}),$$
$$\exp(\Delta t\, X_{p_1})\exp(\Delta t\, X_{p_2}) = \exp(\Delta t\, \tilde{X}_{p_{1,2}}),$$
$$\exp(\Delta t\, \tilde{X}_{p_{1,2}})\exp(h X_{p_3}) = \exp(\Delta t\, \tilde{X}_{p_{1,2,3}}),$$
$$\exp(\Delta t\, \tilde{X}_{EB})\exp(\Delta t\, \tilde{X}_{p_{1,2,3}}) = \exp(\Delta t\, \tilde{X}),$$

where the corresponding Hamiltonians are given by

$$\tilde{\mathcal{H}}_{EB} = \hat{\mathcal{H}}_E + \hat{\mathcal{H}}_B + \frac{h}{2}\{\hat{\mathcal{H}}_E, \hat{\mathcal{H}}_B\} + \mathcal{O}(\Delta t^2),$$

$$\tilde{\mathcal{H}}_{p_{1,2}} = \hat{\mathcal{H}}_{p_1} + \hat{\mathcal{H}}_{p_2} + \frac{h}{2}\{\hat{\mathcal{H}}_{p_1}, \hat{\mathcal{H}}_{p_2}\} + \mathcal{O}(\Delta t^2),$$

$$\tilde{\mathcal{H}}_{p_{1,2,3}} = \tilde{\mathcal{H}}_{p_{1,2}} + \hat{\mathcal{H}}_{p_3} + \frac{h}{2}\{\tilde{\mathcal{H}}_{p_{1,2}}, \hat{\mathcal{H}}_{p_3}\} + \mathcal{O}(\Delta t^2)$$

$$= \hat{\mathcal{H}}_{p_1} + \hat{\mathcal{H}}_{p_2} + \hat{\mathcal{H}}_{p_3} + \frac{h}{2}\{\hat{\mathcal{H}}_{p_1}, \hat{\mathcal{H}}_{p_2}\} + \frac{h}{2}\{\hat{\mathcal{H}}_{p_1} + \hat{\mathcal{H}}_{p_2}, \hat{\mathcal{H}}_{p_3}\} + \mathcal{O}(\Delta t^2).$$

The Hamiltonian $\tilde{\mathcal{H}}$ corresponding to $\tilde{X}$ is given by

$$\tilde{\mathcal{H}} = \hat{\mathcal{H}}_E + \hat{\mathcal{H}}_B + \hat{\mathcal{H}}_{p_1} + \hat{\mathcal{H}}_{p_2} + \hat{\mathcal{H}}_{p_3} + h\tilde{\mathcal{H}}_1 + \mathcal{O}(\Delta t^2), \tag{136}$$

with the first order correction $\tilde{\mathcal{H}}_1$ obtained as

$$\tilde{\mathcal{H}}_1 = \frac{1}{2}\left[\{\hat{\mathcal{H}}_E, \hat{\mathcal{H}}_B\} + \{\hat{\mathcal{H}}_{p_1}, \hat{\mathcal{H}}_{p_2}\} + \{\hat{\mathcal{H}}_{p_1} + \hat{\mathcal{H}}_{p_2}, \hat{\mathcal{H}}_{p_3}\} + \{\hat{\mathcal{H}}_E + \hat{\mathcal{H}}_B, \hat{\mathcal{H}}_p\} \right]. \tag{137}$$

The various Poisson brackets are computed as follows,

$$\{\hat{\mathcal{H}}_E, \hat{\mathcal{H}}_B\} = \mathbf{e}^\top \mathbb{C}^\top \mathbf{b},$$
$$\{\hat{\mathcal{H}}_E, \hat{\mathcal{H}}_p\} = -\mathbf{e}^\top \mathbb{A}^1(\mathbf{X})^\top \mathbb{M}_q \mathbf{V},$$
$$\{\hat{\mathcal{H}}_B, \hat{\mathcal{H}}_p\} = 0,$$
$$\{\hat{\mathcal{H}}_{p_1}, \hat{\mathcal{H}}_{p_2}\} = \mathbf{V}^1 M_q \mathbb{B}^3(\mathbf{b}, \mathbf{X})^\top \mathbf{V}^2,$$
$$\{\hat{\mathcal{H}}_{p_2}, \hat{\mathcal{H}}_{p_3}\} = \mathbf{V}^2 M_q \mathbb{B}^1(\mathbf{b}, \mathbf{X})^\top \mathbf{V}^3,$$
$$\{\hat{\mathcal{H}}_{p_3}, \hat{\mathcal{H}}_{p_1}\} = \mathbf{V}^3 M_q \mathbb{B}^2(\mathbf{b}, \mathbf{X})^\top \mathbf{V}^1,$$

where $\mathbb{B}^\mu(\mathbf{X}, \mathbf{b})$ denotes $N_p \times N_p$ diagonal matrix with elements $B_h^\mu(\mathbf{x}_a)$. The Lie-Trotter integrator (124) preserves the modified energy $\hat{\mathcal{H}} + h\tilde{\mathcal{H}}_1$ to $\mathcal{O}(\Delta t^2)$, while the original energy $\hat{\mathcal{H}}$ is preserved only to $\mathcal{O}(\Delta t)$.

6   Example: Vlasov-Maxwell in 1D2V

In one spatial dimension (x) and two velocity dimensions (v_1, v_2), the Vlasov equation takes the following form

$$\frac{\partial f(x,v,t)}{\partial t} + v_1 \frac{\partial f(x,v,t)}{\partial x} + \frac{q_s}{m_s} \mathbf{E}(x,t) \cdot \nabla_v f(x,v,t) + \frac{q_s}{m_s} B_z(x,t) \begin{pmatrix} v_2 \\ -v_1 \end{pmatrix} \cdot \nabla_v f(x,v,t) = 0, \tag{138}$$

while Maxwell's equations become

$$\begin{aligned}
\frac{\partial B_z(x,t)}{\partial t} &= -\frac{\partial E_y(x,t)}{\partial x}, \\
\frac{\partial E_x(x,t)}{\partial t} &= -j_x(x), \\
\frac{\partial E_y(x,t)}{\partial t} &= -\frac{\partial B_z(x,t)}{\partial x} - j_y(x), \\
\frac{\partial E_x(x,t)}{\partial x} &= \rho.
\end{aligned} \tag{139}$$

Here, we consider the components of the electromagnetic fields separately and we have that E_x is a one-form, E_y is a zero-form and B_z is again a one-form. We denote the semi-discrete fields by D_h, E_h and B_h respectively, and write

$$\begin{aligned}
D_h(x,t) &= \sum_{i=1}^{N_1} d_i(t)\,\Lambda_i^1(x), \\
E_h(x,t) &= \sum_{i=1}^{N_0} e_i(t)\,\Lambda_i^0(x), \\
B_h(x,t) &= \sum_{i=1}^{N_1} b_i(t)\,\Lambda_i^1(x).
\end{aligned} \tag{140}$$

Next we introduce an equidistant grid in x and denote the spline of degree p with support starting at x_i by N_i^p. We can express the derivative of N_i^p as follows

$$\frac{\mathrm{d}}{\mathrm{d}x} N_i^p(x) = \frac{1}{\Delta x}\left(N_i^{p-1}(x) - N_{i+1}^{p-1}(x)\right). \tag{141}$$

In the finite element field solver, we represent E_h by an expansion in splines of order p and D_h, B_h by an expansion in splines of order $p-1$, that is

$$\begin{aligned}
D_h(x,t) &= \sum_{i=1}^{N_1} d_i(t)\,N_i^{p-1}(x), \\
E_h(x,t) &= \sum_{i=1}^{N_0} e_i(t)\,N_i^p(x), \\
B_h(x,t) &= \sum_{i=1}^{N_1} b_i(t)\,N_i^{p-1}(x).
\end{aligned} \tag{142}$$

The Hamiltonian is given in terms of the degrees of freedom $\mathbf{u} = (\mathbf{X}, \mathbf{V}_1, \mathbf{V}_2, \mathbf{d}, \mathbf{e}, \mathbf{b})$ by

$$\hat{\mathcal{H}} = \tfrac{1}{2}\mathbf{V}_1^\top M_p \mathbf{V}_1 + \tfrac{1}{2}\mathbf{V}_2^\top M_p \mathbf{V}_2 + \tfrac{1}{2}\mathbf{d}^\top M_1 \mathbf{d} + \tfrac{1}{2}\mathbf{e}^\top M_0 \mathbf{e} + \tfrac{1}{2}\mathbf{b}^\top M_1 \mathbf{b}. \tag{143}$$

The discrete Poisson bracket (79) for this system reads

$$
\begin{aligned}
\{\hat{F}, \hat{G}\}[\mathbf{X}, \mathbf{V}_1, \mathbf{V}_2, \mathbf{d}, \mathbf{e}, \mathbf{b}] = &\frac{\partial \hat{F}}{\partial \mathbf{V}_1} M_p^{-1} \frac{\partial \hat{G}}{\partial \mathbf{V}_1} - \frac{\partial \hat{G}}{\partial \mathbf{V}_1} M_p^{-1} \frac{\partial \hat{F}}{\partial \mathbf{V}_1} \\
&+ \left(\frac{\partial \hat{F}}{\partial \mathbf{V}_1}\right)^{\top} M_p^{-1} M_q \mathbb{\Lambda}^1(\mathbf{X})^{\top} M_1^{-1} \left(\frac{\partial \hat{G}}{\partial \mathbf{d}}\right) \\
&- \left(\frac{\partial \hat{F}}{\partial \mathbf{d}}\right)^{\top} M_1^{-1} \mathbb{\Lambda}^1(\mathbf{X}) M_q M_p^{-1} \left(\frac{\partial \hat{G}}{\partial \mathbf{V}_1}\right) \\
&+ \left(\frac{\partial \hat{F}}{\partial \mathbf{V}_2}\right)^{\top} M_p^{-1} M_q \mathbb{\Lambda}^0(\mathbf{X})^{\top} M_0^{-1} \left(\frac{\partial \hat{G}}{\partial \mathbf{e}}\right) \\
&- \left(\frac{\partial \hat{F}}{\partial \mathbf{e}}\right)^{\top} M_0^{-1} \mathbb{\Lambda}^0(\mathbf{X}) M_q M_p^{-1} \left(\frac{\partial \hat{G}}{\partial \mathbf{V}_2}\right) \\
&+ \left(\frac{\partial \hat{F}}{\partial \mathbf{V}_1}\right)^{\top} M_p^{-1} M_q \mathbb{B}(\mathbf{X}, \mathbf{b}) M_p^{-1} \left(\frac{\partial \hat{G}}{\partial \mathbf{V}_2}\right) \\
&- \left(\frac{\partial \hat{F}}{\partial \mathbf{V}_2}\right)^{\top} M_p^{-1} \mathbb{B}(\mathbf{X}, \mathbf{b}) M_q M_p^{-1} \left(\frac{\partial \hat{G}}{\partial \mathbf{V}_1}\right) \\
&+ \left(\frac{\partial \hat{F}}{\partial \mathbf{e}}\right)^{\top} M_0^{-1} \mathbb{C}^{\top} M_1^{-1} \left(\frac{\partial \hat{G}}{\partial \mathbf{b}}\right) \\
&- \left(\frac{\partial \hat{F}}{\partial \mathbf{b}}\right)^{\top} M_1^{-1} \mathbb{C} M_0^{-1} \left(\frac{\partial \hat{G}}{\partial \mathbf{e}}\right).
\end{aligned}
\tag{144}
$$

Here, we denote by $\mathbb{\Lambda}^0(\mathbf{X})$ the $N_p \times N_0$ matrix with generic term $\Lambda_i^0(\mathbf{x}_a)$, where $1 \leq a \leq N_p$ and $1 \leq i \leq N_0$, and by $\mathbb{\Lambda}^1(\mathbf{X})$ the $N_p \times N_1$ matrix with generic term $\Lambda_i^1(\mathbf{x}_a)$, where $1 \leq a \leq N_p$ and $1 \leq i \leq N_1$. Further, $\mathbb{B}(\mathbf{X}, \mathbf{b})$ denotes the $N_p \times N_p$ diagonal matrix with entries

$$
B_h(\mathbf{x}_a, t) = \sum_{i=1}^{N_1} b_i(t) \, \Lambda_i^1(\mathbf{x}_a).
\tag{145}
$$

The equations of motion are obtained as follows,

$$
\begin{aligned}
\dot{\mathbf{X}} &= \mathbf{V}_1, \\
\dot{\mathbf{V}}_1 &= M_p^{-1} M_q \big(\mathbb{\Lambda}^1(\mathbf{X})\mathbf{d} + \mathbb{B}(\mathbf{X}, \mathbf{b})\mathbf{V}_2\big), \\
\dot{\mathbf{V}}_2 &= M_p^{-1} M_q \big(\mathbb{\Lambda}^0(\mathbf{X})\mathbf{e} - \mathbb{B}(\mathbf{X}, \mathbf{b})\mathbf{V}_1\big), \\
\dot{\mathbf{d}} &= -M_1^{-1}\mathbb{\Lambda}^1(\mathbf{X})^{\top} M_q \mathbf{V}_1, \\
\dot{\mathbf{e}} &= M_0^{-1}\big(\mathbb{C}^{\top}\mathbf{b}(t) - \mathbb{\Lambda}^0(\mathbf{X})^{\top} M_q \mathbf{V}_2\big), \\
\dot{\mathbf{b}} &= -\mathbb{C}\mathbf{e}(t),
\end{aligned}
\tag{146}
$$

which is seen to be in direct correspondence with (138)-(139).

6.1 Hamiltonian Splitting

The solution of the discrete equations of motion for $\hat{\mathcal{H}}_D + \hat{\mathcal{H}}_E$ at time Δt is

$$
\begin{aligned}
M_p \mathbf{V}_1(\Delta t) &= M_p \mathbf{V}_1(0) + \Delta t \, M_q \mathbb{\Lambda}^1(\mathbf{X}(0)) \, \mathbf{d}(0), \\
M_p \mathbf{V}_2(\Delta t) &= M_p \mathbf{V}_2(0) + \Delta t \, M_q \mathbb{\Lambda}^0(\mathbf{X}(0)) \, \mathbf{e}(0), \\
\mathbf{b}(\Delta t) &= \mathbf{b}(0) - \Delta t \, \mathbb{C} \mathbf{e}(0).
\end{aligned}
\tag{147}
$$

The solution of the discrete equations of motion for $\hat{\mathcal{H}}_B$ is

$$M_0 \mathbf{e}(\Delta t) = M_0 \mathbf{e}(0) + \Delta t\, \mathbb{C}^\top \mathbf{b}(0). \tag{148}$$

The solution of the discrete equations of motion for $\hat{\mathcal{H}}_{p_1}$ is

$$\mathbf{X}(\Delta t) = \mathbf{X}_1(0) + \Delta t\, \mathbf{V}_1(0),$$

$$M_p \mathbf{V}_2(\Delta t) = M_p \mathbf{V}_2(0) - \int_0^{\Delta t} M_q \mathbb{B}(\mathbf{X}(t), \mathbf{b}(0)) \mathbf{V}_1(0)\, \mathrm{d}t, \tag{149}$$

$$M_1 \mathbf{d}(\Delta t) = M_1 \mathbf{d}(0) - \int_0^{\Delta t} \mathbb{A}^1(\mathbf{X}(t))^\top M_q \mathbf{V}_1(0)\, \mathrm{d}t,$$

and for $\hat{\mathcal{H}}_{p_2}$ it is

$$M_p \mathbf{V}_1(\Delta t) = M_p \mathbf{V}_1(0) + \int_0^{\Delta t} M_q \mathbb{B}(\mathbf{X}(0), \mathbf{b}(0)) \mathbf{V}_2(0)\, \mathrm{d}t,$$

$$M_0 \mathbf{e}(\Delta t) = M_0 \mathbf{e}(0) - \int_0^{\Delta t} \mathbb{A}^1(\mathbf{X}(0))^\top M_q \mathbf{V}_2(0)\, \mathrm{d}t, \tag{150}$$

respectively.

6.2 Boris-Yee scheme

As an alternative discretization scheme, we consider a Boris-Yee scheme [9, 81] with our conforming finite elements. The scheme uses a time staggering working with the variables $\mathbf{X}^{n+1/2} = \mathbf{X}(t^n + \Delta t/2)$, $\mathbf{d}^{n+1/2} = \mathbf{d}(t^n + \Delta t/2)$, $\mathbf{e}^{n+1/2} = \mathbf{e}(t^n + \Delta t/2)$, $\mathbf{V}^n = \mathbf{V}(t^n)$, and $\mathbf{b}^n = \mathbf{b}(t^n)$ in the nth time step $t^n = t^0 + n\Delta t$. The Hamiltonian at time t^n is defined as

$$\hat{\mathcal{H}} = \tfrac{1}{2} \left(\mathbf{V}_1^n\right)^\top M_p \mathbf{V}_1^n + \tfrac{1}{2} \left(\mathbf{V}_2^n\right)^\top M_p \mathbf{V}_2^n + \tfrac{1}{2} \left(\mathbf{d}^{n-1/2}\right)^\top M_1 \mathbf{d}^{n+1/2}$$
$$+ \tfrac{1}{2} \left(\mathbf{e}^{n-1/2}\right)^\top M_0 \mathbf{e}^{n+1/2} + \tfrac{1}{2} \left(\mathbf{b}^n\right)^\top M_1 \mathbf{b}^n. \tag{151}$$

Given $\mathbf{X}^{n-1/2}$, $\mathbf{d}^{n-1/2}$, $\mathbf{e}^{n-1/2}$, $\mathbf{V}^{n-1}$, $\mathbf{b}^{n-1}$ the Vlasov-Maxwell system is propagated by the following time step:

1. Compute $\mathbf{b}^n$ according to

$$b_i^n = b_i^{n-1} - \frac{\Delta t}{\Delta x} \left(e_i^{n-1/2} - e_{i-1}^{n-1/2} \right). \tag{152}$$

   and $\mathbf{b}^{n-1/2} = (\mathbf{b}^{n-1} + \mathbf{b}^n)/2$.

2. Propagate $\mathrm{v}^{n-1} \to \mathrm{v}^n$ by equation

$$\mathrm{v}_a^- = \mathrm{v}_a^{n-1} + \frac{\Delta t}{2} \frac{q_s}{m_s} D^{n-1/2}(\mathrm{x}_a^{n-1/2}), \tag{153}$$

$$\mathrm{v}_a^+ = \mathrm{v}_a^- + \frac{\Delta t}{2} \frac{q_s}{m_s} (\mathrm{v}_a^+ + \mathrm{v}_a^-) \times B^{n-1/2}(\mathrm{x}_a^{n-1/2}), \tag{154}$$

$$\mathrm{v}_a^n = \mathrm{v}_a^+ + \frac{\Delta t}{2} \frac{q_s}{m_s} D^{n-1/2}(\mathrm{x}_a^{n-1/2}). \tag{155}$$

3. Propagate $\mathrm{x}^{n-1/2} \to \mathrm{x}^{n+1/2}$ by

$$\mathrm{x}_a^{n+1/2} = \mathrm{x}_a^{n-1/2} + \Delta t\, \mathrm{v}_{1,a}^n. \tag{156}$$

and accumulate $\mathbf{j}_x^n$, $\mathbf{j}_y^n$ by

$$\mathbf{j}_x^n = \sum_{a=1}^{N_p} w_a \mathrm{v}_{1,a}^n \Lambda^1 \left((\mathrm{x}_a^{n-1/2} + \mathrm{x}_a^{n+1/2})/2 \right), \tag{157}$$

$$\mathbf{j}_y^n = \sum_{a=1}^{N_p} w_a \mathrm{v}_{2,a}^n \Lambda^0 \left((\mathrm{x}_a^{n-1/2} + \mathrm{x}_a^{n+1/2})/2 \right). \tag{158}$$

4. Compute $\mathbf{d}^{n+1/2}$ according to

$$M_1 \mathbf{d}^{n+1/2} = M_1 \mathbf{d}^{n-1/2} - \Delta t\, \mathbf{j}_x^n, \tag{159}$$

and $\mathbf{e}^{n+1/2}$ according to

$$M_0 \mathbf{e}^{n+1/2} = M_0 \mathbf{e}^{n-1/2} + \frac{\Delta t}{\Delta x} \mathbb{C}^T \mathbf{b}^n - \Delta t\, \mathbf{j}_y^n. \tag{160}$$

For the initialisation, we sample $\mathbf{X}^0$ and $\mathbf{V}^0$ from the initial sampling distribution, set $\mathbf{e}^0$, $\mathbf{b}^0$ from the given initial fields, and solve Poisson's equation for $\mathbf{d}^0$. Then, we compute $\mathbf{X}^{1/2}$, $\mathbf{d}^{1/2}$, and $\mathbf{e}^{1/2}$ from the corresponding equations of the Boris-Yee scheme for a half time step, using $\mathbf{b}^0$, $\mathbf{V}^0$ instead of the unknown values at time $\Delta t/4$. Note that the error in this step is of order Δt^2. But since we only introduce this error in the first time step, the overall scheme is still of order two.

7 Numerical Experiments

We have implemented the Hamiltonian splitting scheme as well as the Boris-Yee scheme as part of the SeLaLib library [1]. In this section, we present results for various test cases in 1d2v, comparing the conservation properties of total energy and of the Casimir for the two schemes. We simulate the electron distribution function in a neutralizing ion background. In all experiments, we have used splines of order three for the 0-forms. The particle loading was done using Sobol numbers and antithetic sampling (symmetric around the middle of the domain in x and around the mean value of the Gaussian from which we are sampling in each velocity dimension). We sample uniformly in x and from the Gaussians of the initial distribution in each velocity dimension.

7.1 Weibel instability

We consider the Weibel instability studied in Weibel [77] in the form simulated in [29]. We study a reduced 1d2v model with a perturbation along x_1, a magnetic field along x_3 and electric fields along the x_1 and x_2 directions. Moreover, we assume that the distribution function is independent of v_3. The initial distribution and fields are of the form

Table 1: Weibel instability: Maximum error in the total energy and Poisson's equation until time 500 for simulation with various integrators.

Propagator	total energy	Poisson
Lie	4.9E-7	8.7E-15
Strang	6.3E-7	1.5E-14
2nd, 4 Lie	9.8E-7	1.6E-14
4th, 3 Strang	2.1E-9	2.2E-14
4th, 10 Lie	2.1E-13	3.9E-14
Boris	3.4E-10	1.0E-4

$$f(x_1, v_1, v_2, t = 0) = \frac{1}{\pi \sigma_1 \sigma_2} \exp\left(-\frac{1}{2}\left(\frac{v_1^2}{\sigma_1^2} + \frac{v_2^2}{\sigma_2^2}\right)\right)(1 + \alpha \cos(kx)), \quad x_1 \in [0, 2\pi/k],$$
(161)

$$B_3(x_1, t = 0) = \beta \cos(kx),$$
(162)

$$E_2(x_1, t = 0) = 0,$$
(163)

and $E_1(x_1, t = 0)$ is computed from Poisson's equation.

In our simulations, we use the following choice of parameters, $\sigma_1 = 0.02/\sqrt{2}$, $\sigma_2 = \sqrt{12}\sigma_1$, $k = 1.25$, $\alpha = 0$, and $\beta = -10^{-4}$. Note that these are the same parameters as in [29] except for the fact that we sample from the Maxwellian without perturbation in x_1. However, we will have a perturbation due to the numerical noise.

The dispersion relation from [77] applied to our model choices reads

$$D(\omega, k) = \omega^2 - k^2 + \left(\frac{\sigma_2}{\sigma_1}\right)^2 - 1 - \left(\frac{\sigma_2}{\sigma_1}\right)^2 \phi\left(\frac{\omega}{\sigma_1 k}\right)\frac{\omega}{\sigma_1 k},$$
(164)

where $\phi(z) = \exp\left(-\frac{1}{2}z^2\right)\int_{-i\infty}^{z} \exp\left(\frac{1}{2}\xi^2\right) d\xi$. For our parameter choice, this gives a growth rate of 0.02784. In Figure 1, we show the electric and magnetic energies together with the analytic growth rate. We see that the growth rate is verified in the numerical solution. This simulation was performed with 100,000 particles, 32 grid points, splines of degree 3 and 2 and $\Delta t = 0.05$.

In Table 1, we show the conservation properties of our splitting with various order of the splitting and compare them also to the Boris–Yee scheme. The other numerical parameters are kept as before.

We can see that the Poisson equation is satisfied in each time step for the Hamiltonian splitting. This is a Casimir (cf. Sec. **??** and therefore naturally conserved by the Hamiltonian splitting. On the other hand, this is not the case for the Boris–Yee scheme.

We can also see that the energy error improves with the order of the splitting but the Hamiltonian splitting method as well as the Boris-Yee scheme are not energy conserving. The time evolution of the total energy error is depicted in Figure 2 for the various methods.

7.2 Streaming Weibel instability

As a second test case, we consider the streaming Weibel instability. We study the same reduced model as in the previous section but following [17, 26], the initial distribution
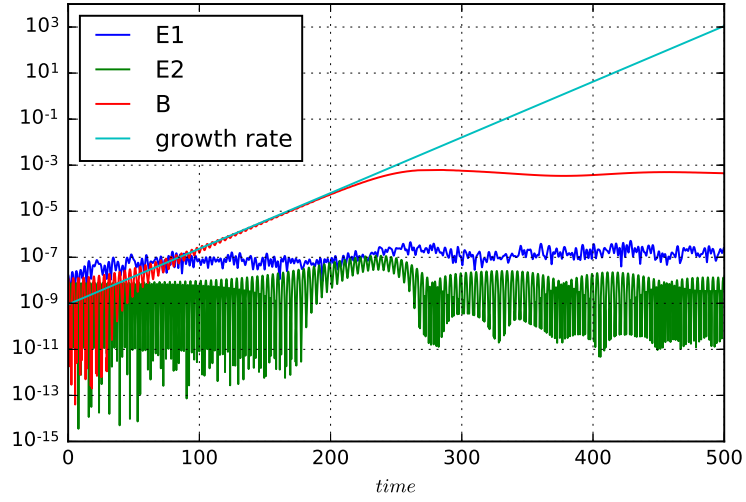
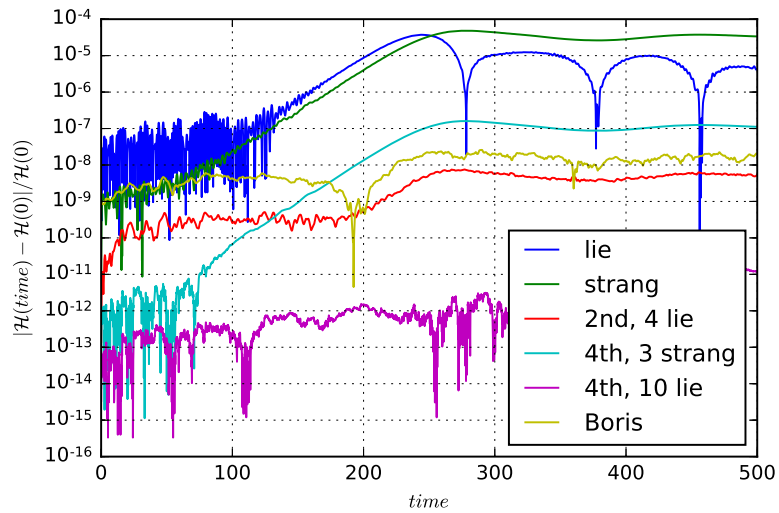Figure 1: Weibel instablity: The two electric and the magnetic energies together with the analytic growth rate.

Figure 2: Weibel instablity: Difference of total energy to initial value as a function of time for various integators.

32

Table 2: Streaming Weibel instability: Maximum error in the total energy and Poisson's equation until time 500 for simulation with various integrators.

Propagator	total energy	Poisson
Lie	6.4E-5	8.3E-15
Strang	1.4E-6	1.4E-14
2nd, 4 Lie	1.5E-8	2.0E-14
4th, 3 Strang	1.7E-10	9.4E-15
4th, 10 Lie	5.7E-13	1.0E-14
Boris	1.1E-7	5.8E-4

and fields are prescribed as

$$f(x, v_1, v_2, t = 0) = \frac{1}{\pi\sigma} \exp\left(-\frac{v_1^2}{2\sigma^2}\right)\left(\delta \exp\left(-\frac{(v_2 - v_{0,1})^2}{2\sigma^2}\right)\right.$$
$$\left. + (1 - \delta) \exp\left(-\frac{(v_2 - v_{0,2})^2}{2\sigma^2}\right)\right), \quad (165)$$

$$B_3(x, t = 0) = \beta \sin(kx), \quad (166)$$
$$E_2(x, t = 0) = 0, \quad (167)$$

and $E_1(x, t = 0)$ is computed from Poisson's equation.

We set the parameters to the following values $\sigma = 0.1/\sqrt{2}$, $k = 0.2$, $\beta = -10^{-3}$, $v_{0,1} = 0.5$, $v_{0,2} = -0.1$ and $\delta = 1/6$. The parameters are chosen as in the case 2 of [26]. The growth rate of energy of the second component of the electric field was determined to be 0.03 in [17]. In Figure 3, we show the electric and magnetic energies together with the analytic growth rate. We see that the growth rate is verified in the numerical solution. This simulation was performed on the domain $x \in [0, 2\pi/k)$ with 2,000,000 particles, 128 grid points, splines of degree 3 and 2 and $\Delta t = 0.01$.

As for the Weibel instability, we compare the conservation properties in Table 2 for various integrators. Again we see that the Hamiltonian splitting conserves the Poisson equation as opposed to the Boris–Yee scheme. The energy conservation properties of the various scheme show about the same behavior as in the previous test case (see also Fig. 4 for the time evolution of the energy error).
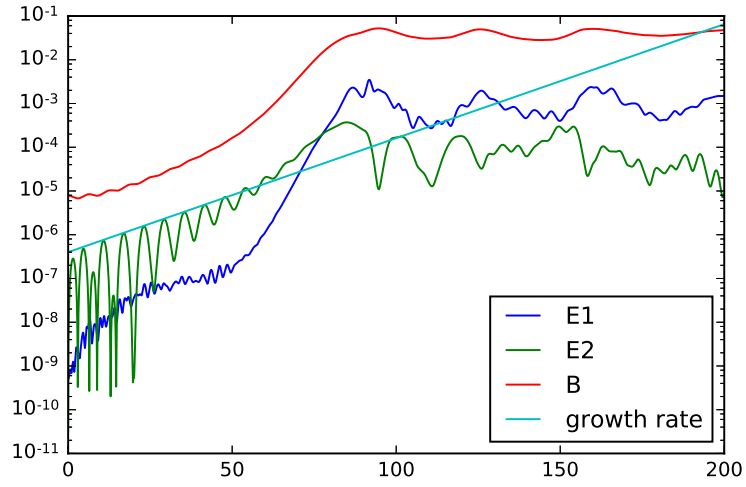
Figure 3: Streaming Weibel instablity: The two electric and the magnetic energies together with the analytic growth rate.
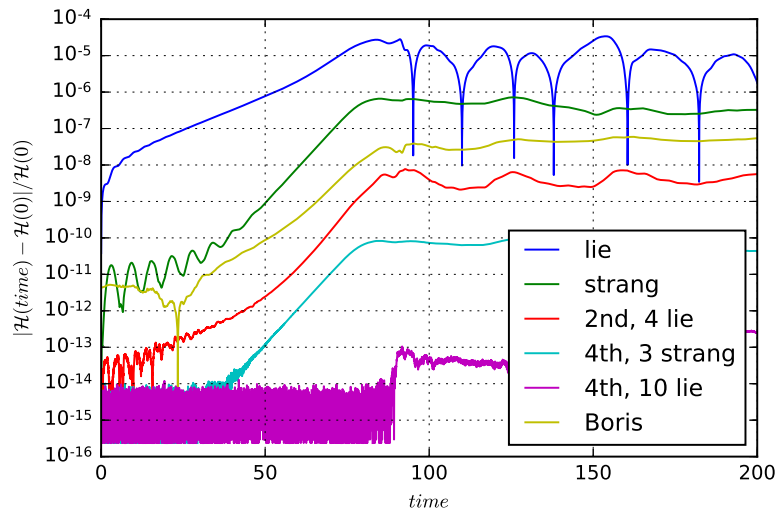

Figure 4: Streaming Weibel instablity: Difference of total energy to initial value as a function of time for various integrators.
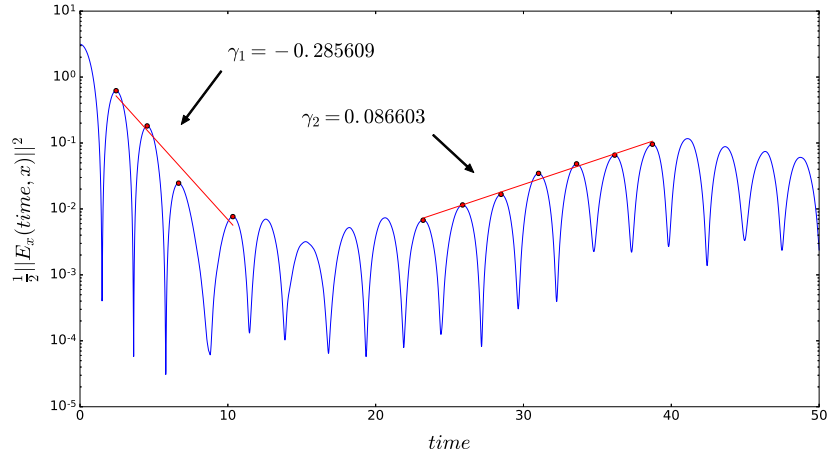
Figure 5: Landau damping: Electric energy with fitted growth rates.

7.3 Strong Landau damping

Finally, we also study the electrostatic example of strong Landau damping with initial distribution

$$f(x, v_1, v_2) = \exp\left(-\frac{v_1^2 + v_2^2}{2\sigma^2}\right)\left(1 + A\cos(kx)\right). \tag{168}$$

The physical parameters are chosen as $\sigma = 1$, $k = 0.5$, $A = 0.5$ and the numerical parameters as $x \in [0, 2\pi/k)$, $v \in \mathbb{R}^2$, $\Delta t = 0.01$, $n_x = 32$. The fields B and E_2 are initialized to zero and remain zero over time. In this example, we essentially solve the Vlasov–Ampère equation with results equivalent to the Vlasov–Poisson equations. In Figure 5, we show the time evolution of the electric energy. We have also fitted a damping and growth rate (using the marked local maxima in the plot). These are well in agreement with other codes (see Table 3). Again the energy conservation for the various method is visualized as a function of time in Figure 6. Again we see that the fourth order methods give excellent energy conservation.

7.4 Backward Error Analysis

For the Lie-Trotter splitting, the error in the Hamiltonian $\hat{\mathcal{H}}$ is of order Δt. However, using backward error analysis (cf. Section 5.3), modified Hamiltonians can be computed, which are preserved to higher order. Accounting for first order corrections $\tilde{\mathcal{H}}_1$, the error

Table 3: Damping and growth rates for strong Landau damping.

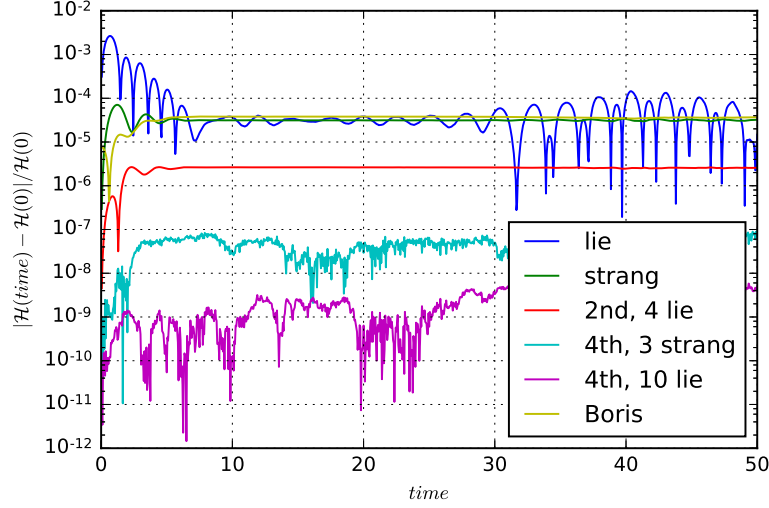| Integrator	γ_1	γ_2
GEMPIC	-0.286	$+0.087$
viVlasov1D [45]	-0.286	$+0.085$
Cheng & Knorr [22]	-0.281	$+0.084$
Nakamura & Yabe [64]	-0.280	$+0.085$
Ayuso & Hajian [31]	-0.292	$+0.086$
Heath, Gamba, Morrison, Michler [42]	-0.287	$+0.075$
Cheng, Gamba, Morrison [23]	-0.291	$+0.086$

Figure 6: Landau damping: Electric energy with fitted growth rates.

in the modified Hamiltonian,

$$\tilde{\mathcal{H}} = \hat{\mathcal{H}} + h\tilde{\mathcal{H}}_1 + \mathcal{O}(\Delta t^2), \tag{169}$$

is of order $(\Delta t)^2$. For the 1d2v example, this correction is obtained as

$$\tilde{\mathcal{H}}_1 = \frac{1}{2} \left[\{\hat{\mathcal{H}}_D + \hat{\mathcal{H}}_E, \hat{\mathcal{H}}_B\} + \{\hat{\mathcal{H}}_{p_1}, \hat{\mathcal{H}}_{p_2}\} + \{\hat{\mathcal{H}}_D + \hat{\mathcal{H}}_E + \hat{\mathcal{H}}_B, \hat{\mathcal{H}}_{p_1} + \hat{\mathcal{H}}_{p_2}\} \right], \tag{170}$$

with the various Poisson brackets computed as

$$\{\hat{\mathcal{H}}_D, \hat{\mathcal{H}}_B\} = 0,$$
$$\{\hat{\mathcal{H}}_E, \hat{\mathcal{H}}_B\} = \mathbf{e}^\top \mathbb{C}^\top \mathbf{b},$$
$$\{\hat{\mathcal{H}}_{p1}, \hat{\mathcal{H}}_{p2}\} = \mathbf{V}^1 M_q \mathbb{B}(\mathbf{b}, \mathbf{X})^\top \mathbf{V}^2,$$
$$\{\hat{\mathcal{H}}_D, \hat{\mathcal{H}}_{p1}\} = -\mathbf{d}^\top \mathbb{A}^1(\mathbf{X})^\top M_q \mathbf{V}^1,$$
$$\{\hat{\mathcal{H}}_D, \hat{\mathcal{H}}_{p2}\} = 0,$$
$$\{\hat{\mathcal{H}}_E, \hat{\mathcal{H}}_{p1}\} = 0,$$
$$\{\hat{\mathcal{H}}_E, \hat{\mathcal{H}}_{p2}\} = -\mathbf{e}^\top \mathbb{A}^0(\mathbf{X})^\top M_q \mathbf{V}^2,$$
$$\{\hat{\mathcal{H}}_B, \hat{\mathcal{H}}_{p1}\} = 0,$$
$$\{\hat{\mathcal{H}}_B, \hat{\mathcal{H}}_{p2}\} = 0.$$

In Figure 7, we show the maximum and l2 error of the energy and the corrected energy for the Weibel instability test case with the parameters in Sec. 7.1. The simulations were performed with 100,000 particles, 32 grid points, splines of degree 3 and 2 and $\Delta t = 0.01, 0.02, 0.05$. We can see that the theoretical convergence rates are verified in the numerical experiments. Figure 8 shows the energy as well as the modified energy for the Weibel instability test case simulated with a time step of 0.05.
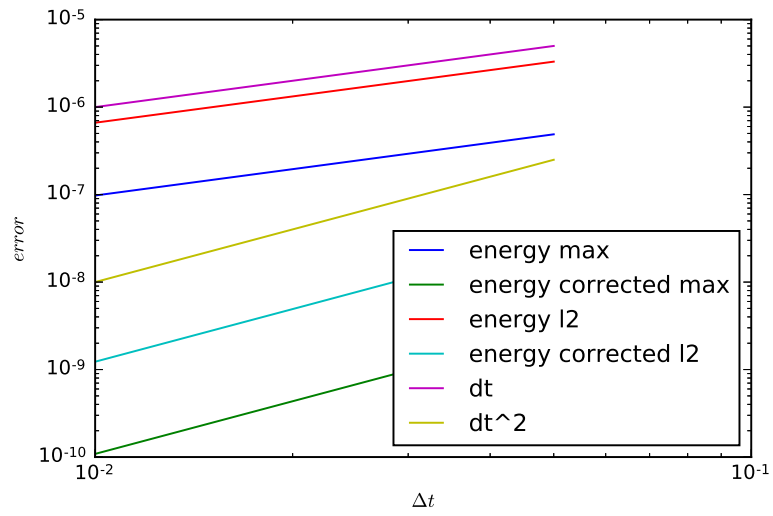
Figure 7: Weibel instability: Error (maximum norm and l2 norm) in the total energy for simulations with $\Delta t = 0.01, 0.02, 0.05$.
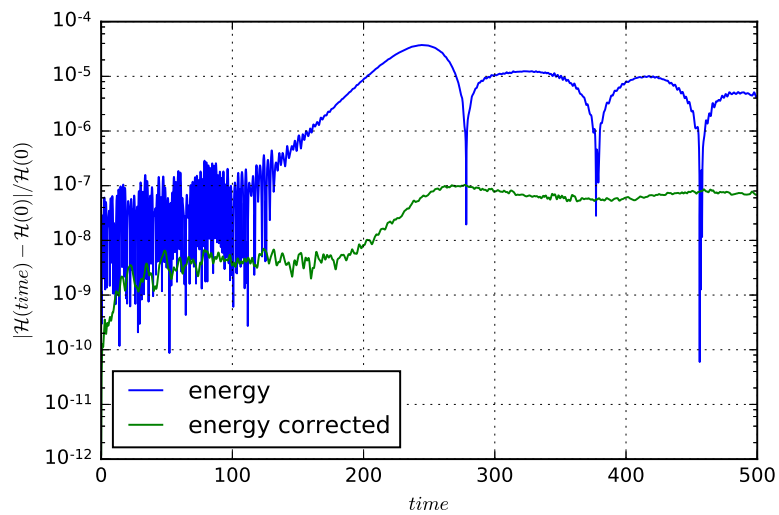

Figure 8: Weibel instability: Energy and first-order corrected energy for simulation with $\Delta t = 0.05$.

8 Summary

In this work, a general framework for geometric Finite Element Particle-in-Cell methods for the Vlasov-Maxwell system was presented. The discretization proceeded in two steps. First, a semi-discretization of the noncanonical Lie-Poisson bracket was obtained, which preserves the Jacobi identity and important Casimirs. Then, the system was discretised in time by Hamiltonian splitting methods, still retaining exact conservation of Casimirs. Energy was not preserved, but backward error analysis showed that the energy error does not depend on the degrees of freedom, the number of particles or the number time steps. The favorable properties of the method were verified in various numerical experiments.

The generality of the framework opens up several new paths for consecutive research. Instead of splines, other finite element spaces which form a deRham sequence could be used, e.g., mimetic spectral elements or Nédélec elements for one-forms and Raviart-Thomas elements for two-forms. Instead of Hamiltonian splitting algorithms, one could use Poisson splitting algorithms, where not the Hamiltonian but the Poisson matrix is split into a sum of matrices. Using an appropriate splitting, the resulting methods will be energy-preserving and could still preserve Casimirs. This is a topic currently under investigation. Further, it should be possible to apply this approach also to other systems like the gyrokinetic Vlasov-Maxwell system [16], although in this case the necessity for new splitting schemes might arise.

Acknowledgments

References

[1] SeLaLib. http://selalib.gforge.inria.fr/.

[2] Douglas N. Arnold, Richard S. Falk, and Ragnar Winther. Finite element exterior calculus, homological techniques, and applications. *Acta Numerica*, 15:1–155, 2006. doi: 10.1017/S0962492906210018.

[3] Douglas N. Arnold, Richard S. Falk, and Ragnar Winther. Finite element exterior calculus: From hodge theory to numerical stability. *Bulletin of the American Mathematical Society*, 47:281–354, 2010. doi: 10.1090/S0273-0979-10-01278-4.

[4] Aurore Back and Eric Sonnendrücker. Finite Element Hodge for spline discrete differential forms. Application to the Vlasov–Poisson system. *Applied Numerical Mathematics*, 79:124–136, 2014.

[5] John Baez and Javier P. Muniain. *Gauge Fields, Knots and Gravity*. World Scientific, 1994.

[6] R. Barthelmé and C. Parzani. Numerical charge conservation in particle-in-cell codes. *Numerical Methods for Hyperbolic and Kinetic Problems*, pages 7–28, 2005.

[7] D. Boffi. Compatible Discretizations for Eigenvalue Problems. In *Compatible Spatial Discretizations*, pages 121–142. Springer New York, NY, 2006.

[8] D. Boffi. Finite element approximation of eigenvalue problems. *Acta Numerica*, 19: 1–120, 2010.

[9] Jay P. Boris. Relativistic plasma-simulation - optimization of a hybrid code. In *Proceedings of the Fourth Conference on Numerical Simulation of Plasmas*, pages 3–67. Naval Research Laboratory, Washington DC, 1970.

[10] J.P. Boris. Relativistic plasma simulations - optimization of a hybrid code. In *Proc. 4th Conf. Num. Sim. of Plasmas, (NRL Washington, Washington DC)*, pages 3–67, 1970.

[11] Alain Bossavit. Differential geometry for the student of numerical methods in electromagnetism, 1990. Lecture notes. Available online on http://butler.cc.tut.fi/~bossavit/Books/DGSNME/DGSNME.pdf.

[12] Alain Bossavit. Applied differential geometry, 2006. Lecture notes. Available online on http://butler.cc.tut.fi/~bossavit/BackupICM/Compendium.html.

[13] A. Buffa and I. Perugia. Discontinuous Galerkin approximation of the Maxwell eigenproblem. *SIAM Journal on Numerical Analysis*, 44:2198–2226, 2006.

[14] A. Buffa, G. Sangalli, and R. Vázquez. Isogeometric analysis in electromagnetics: B-splines approximation. *Computer Methods in Applied Mechanics and Engineering*, 199(17):1143–1152, 2010.

[15] A. Buffa, J. Rivas, G. Sangalli, and R. Vázquez. Isogeometric discrete differential forms in three dimensions. *SIAM Journal on Numerical Analysis*, 49:818–844, 2011. doi: 10.1137/100786708.

[16] Joshua W. Burby, Alain J. Brizard, Philip J. Morrison, and Hong Qin. Hamiltonian Gyrokinetic Vlasov–Maxwell system. *Physics Letters A*, 379(36):2073–2077, 2015.

[17] F. Califano, F. Pegoraro, and S. V. Bulanov. Spatial structure and time evolution of the weibel instability in collisionless inhomogeneous plasmas. *Phys. Rev. E*, 56: 963–969, 1997. doi: 10.1103/PhysRevE.56.963.

[18] M. Campos Pinto, S. Jund, S. Salmon, and E. Sonnendrücker. Charge conserving fem-pic schemes on general grids. *C.R. Mecanique*, 342(10-11):570–582, 2014.

[19] S. Caorsi, P. Fernandes, and M. Raffetto. On the convergence of Galerkin finite element approximations of electromagnetic eigenproblems. *SIAM Journal on Numerical Analysis*, 38:580–607, 2000.

[20] Hernán Cendra, Darryl D. Holm, Mark J. W. Hoyle, and Jerrold E. Marsden. The Maxwell–Vlasov Equations in Euler–Poincaré Form. *Journal of Mathematical Physics*, 39:3138 – 3157, 1998. doi: 10.1063/1.532244.

[21] Cristel Chandre, Loïc Guillebon, Aurore Back, Emanuele Tassi, and Philip J. Morrison. On the use of projectors for Hamiltonian systems and their relationship with Dirac brackets. *Journal of Physics A: Mathematical and Theoretical*, 46:125203, 2013. doi: 10.1088/1751-8113/46/12/125203.

[22] C. Z. Cheng and Georg Knorr. The integration of the Vlasov equation in configuration space. *Journal of Computational Physics*, 22:330–351, 1976. doi: 10.1016/0021-9991(76)90053-X.

[23] Yingda Cheng, Irene M. Gamba, and Philip J. Morrison. Study of conservation and recurrence of runge–kutta discontinuous galerkin schemes for vlasov–poisson systems. *Journal of Scientific Computing*, 56:319–349, 2013. doi: 10.1007/s10915-012-9680-x.

[24] Yingda Cheng, Andrew J. Christlieb, and Xinghui Zhong. Energy-conserving discontinuous Galerkin methods for the Vlasov–Ampère system. *Journal of Computational Physics*, 256:630–655, 2014.

[25] Yingda Cheng, Andrew J. Christlieb, and Xinghui Zhong. Energy-conserving discontinuous Galerkin methods for the Vlasov–Maxwell system. *Journal of Computational Physics*, 279:145–173, 2014.

[26] Yingda Cheng, Irene M Gamba, Fengyan Li, and Philip J. Morrison. Discontinuous galerkin methods for the vlasov–maxwell equations. *SIAM Journal on Numerical Analysis*, 52(2):1017–1049, 2014.

[27] Snorre H. Christiansen, Hans Z. Munthe-Kaas, and Brynjulf Owren. Topics in structure-preserving discretization. *Acta Numerica*, 20:1–119, 2011. doi: 10.1017/S096249291100002X.

[28] N. Crouseilles, P. Navaro, and E. Sonnendrücker. Charge conserving grid based methods for the Vlasov-Maxwell equations. *C. R. Mecanique*, 342(10-11):636–646, 2014.

[29] Nicolas Crouseilles, Lukas Einkemmer, and Erwan Faou. Hamiltonian splitting for the Vlasov–Maxwell equations. *Journal of Computational Physics*, 283:224–240, 2015.

[30] Richard W. R. Darling. *Differential Forms and Connections*. Cambridge University Press, 1994.

[31] Blanca Ayuso de Dios and Soheil Hajian. High order and energy preserving discontinuous galerkin methods for the vlasov-poisson system. arXiv:1209.4025, 2012.

[32] Blanca Ayuso de Dios, José A Carrillo, and Chi-Wang Shu. Discontinuous Galerkin Methods For The Multi–Dimensional Vlasov–Poisson Problem. *Mathematical Models and Methods in Applied Sciences*, 22:1250042, 2012.

[33] Mathieu Desbrun, Eva Kanso, and Yiying Tong. *Discrete Differential Geometry*, chapter Discrete Differential Forms for Computational Modeling, pages 287–324. Birkhäuser Basel, 2008. ISBN 978-3-7643-8621-4. doi: 10.1007/978-3-7643-8621-4_16.

[34] Tevian Dray. *Differential Forms and the Geometry of General Relativity.* CRC Press, 2014.

[35] J.W. Eastwood. The virtual particle electromagnetic particle-mesh method. *Computer Physics Communications*, 64(2):252–266, 1991.

[36] T.Zh. Esirkepov. Exact charge conservation scheme for particle-in-cell simulation with an arbitrary form-factor. *Computer Physics Communications*, 135(2):144–153, 2001.

[37] E. G. Evstatiev and B. A. Shadwick. Variational formulation of particle algorithms for kinetic plasma simulations. *Journal of Computational Physics*, 245:376–398, 2013.

[38] Marc Gerritsma. An Introduction to a Compatible Spectral Discretization Method. *Mechanics of Advanced Materials and Structures*, 19:48–67, 2012.

[39] Ernst Hairer, Christian Lubich, and Gerhard Wanner. *Geometric Numerical Integration.* Springer, 2006.

[40] Yang He, Hong Qin, Yajuan Sun, Jianyuan Xiao, Ruili Zhang, and Jian Liu. Hamiltonian integration methods for Vlasov-Maxwell equations. *Physics of Plasmas*, 22:124503, 2015. doi: 10.1063/1.4938034.

[41] Yang He, Yajuan Sun, Hong Qin, and Jian Liu. Hamiltonian particle-in-cell methods for vlasov-maxwell equations. *arXiv preprint arXiv:1606.05716*, 2016.

[42] R. E. Heath, Irene M. Gamba, Philip J. Morrison, and C. Michler. A discontinuous galerkin method for the vlasov–poisson system. *Journal of Computational Physics*, 231:1140–1174, 2012. doi: 10.1016/j.jcp.2011.09.020.

[43] J.S. Hesthaven and T. Warburton. High-order nodal discontinuous Galerkin methods for the Maxwell eigenvalue problem. *Philosophical Transactions of the Royal Society A: Mathematical, Physical and Engineering Sciences*, 362(1816):493–524, March 2004.

[44] Anil N. Hirani. *Discrete Exterior Calculus.* PhD thesis, California Institute of Technology, 2003. URL http://resolver.caltech.edu/CaltechETD:etd-05202003-095403.

[45] Michael Kraus, Omar Maj, and Eric Sonnendrücker. Variational Integrators for the Vlasov-Poisson System. In preparation., 2016.

[46] Jasper Kreeft, Artur Palha, and Marc Gerritsma. Mimetic framework on curvilinear quadrilaterals of arbitrary order. *arXiv preprint arXiv:1111.4304*, 2011.

[47] A.B. Langdon. On enforcing Gauss' law in electromagnetic particle-in-cell codes. *Comput. Phys. Comm.*, 70:447–450, 1992.

[48] FE Low. A Lagrangian Formulation of the Boltzmann-Vlasov Equation for Plasmas. In *Proceedings of the Royal Society of London. Series A, Mathematical and Physical Sciences*, volume 248, pages 282–287, 1958.

[49] Éric Madaule, Marco Restelli, and Eric Sonnendrücker. Energy conserving discontinuous Galerkin spectral element method for the Vlasov–Poisson system. *Journal of Computational Physics*, 279:261–288, 2014.

[50] B. Marder. A method for incorporating Gauss's law into electromagnetic PIC codes. *J. Comput. Phys.*, 68:48–55, 1987.

[51] Jerrold E. Marsden and Alan Weinstein. The Hamiltonian structure of the Maxwell-Vlasov equations. *Physica D: Nonlinear Phenomena*, 4(3):394–406, 1982. doi: 10.1016/0167-2789(82)90043-4.

[52] Robert I. McLachlan and G. Reinout W. Quispel. Splitting methods. *Acta Numerica*, 11:341–434, 2002.

[53] Peter Monk. *Finite Element Methods for Maxwell's Equations*. Oxford University Press, 2003.

[54] H. Moon, F.L. Teixeira, and Y.A. Omelchenko. Exact charge-conserving scatter–gather algorithm for particle-in-cell simulations on unstructured grids: A geometric perspective. *Computer Physics Communications*, 194:43–53, 2015.

[55] Shigeyuki Morita. *Geometry of Differential Forms*. American Mathematical Society, 2001.

[56] P. J. Morrison. Hamiltonian description of the ideal fluid. *Rev. Mod. Phys.*, 70:467–521, Apr 1998. doi: 10.1103/RevModPhys.70.467. URL http://link.aps.org/doi/10.1103/RevModPhys.70.467.

[57] P. J. Morrison. A general theory for gauge-free lifting. *Physics of Plasmas*, 20(1):012104, 2013. doi: http://dx.doi.org/10.1063/1.4774063. URL http://scitation.aip.org/content/aip/journal/pop/20/1/10.1063/1.4774063.

[58] Philip J. Morrison. The Maxwell-Vlasov equations as a continuous hamiltonian system. *Physics Letters A*, 80(5-6):383–386, 1980. doi: 10.1016/0375-9601(80)90776-8.

[59] Philip J. Morrison. Poisson brackets for fluids and plasmas. In *AIP Conference Proceedings*, volume 88, pages 13–46. AIP, 1982.

[60] Philip J. Morrison. Variational Principle and Stability of Nonmonotonic Vlasov-Poisson Equilibria. *Zeitschrift für Naturforschung A*, 42:1115–1123, 1987.

[61] Philip J. Morrison and Dieter Pfirsch. Free-energy expressions for Vlasov equilibria. *Physical Review A*, 40:3898–3910, 1989.

[62] C.-D. Munz, R. Schneider, E. Sonnendrücker, and U. Voß. Maxwell's equations when the charge conservation is not satisfied. *Comptes Rendus de l'Académie des Sciences-Series I-Mathematics*, 328(5):431–436, 1999.

[63] C.-D. Munz, P. Omnes, R. Schneider, E. Sonnendrücker, and U. Voss. Divergence correction techniques for Maxwell solvers based on a hyperbolic model. *Journal of Computational Physics*, 161:484–511, 2000.

[64] Takashi Nakamura and Takashi Yabe. Cubic interpolated propagation scheme for solving the hyper–dimensional vlasov–poisson equation in phase space. *Journal of Computational Physics*, 120:122–154, 1999. doi: 10.1016/S0010-4655(99)00247-7.

[65] Artur Palha, Pedro Pinto Rebelo, René Hiemstra, Jasper Kreeft, and Marc Gerritsma. Physics-compatible discretization techniques on single and dual grids, with application to the Poisson equation of volume forms. *Journal of Computational Physics*, 257:1394–1422, 2014.

[66] Hong Qin, Yang He, Ruili Zhang, Jian Liu, Jianyuan Xiao, and Yulei Wang. Comment on "Hamiltonian splitting for the Vlasov-Maxwell equations". *Journal of Computational Physics*, 297:721–723, 2015. doi: 10.1016/j.jcp.2015.04.056.

[67] Ahmed Ratnani and Eric Sonnendrücker. An arbitrary high-order spline finite element solver for the time domain Maxwell equations. *Journal of Scientific Computing*, 51(1):87–106, 2012. doi: 10.1007/s10915-011-9500-8.

[68] Chi-Wang Shu, José Carrillo, and Blanca Ayuso. Discontinuous Galerkin methods for the one–dimensional Vlasov–Poisson system. *Kinetic and Related Models*, 4:955–989, 2011.

[69] N.J. Sircombe and T.D. Arber. VALIS: A split-conservative scheme for the relativistic 2D Vlasov-Maxwell system. *J. Comput. Phys.*, 228:4773–4788, 2009.

[70] Eric Sonnendrücker. *Numerical Methods for the Vlasov-Maxwell Equations*. Springer, 2016.

[71] J. Squire, H. Qin, and W. M. Tang. Geometric integration of the Vlasov–Maxwell system with a variational particle–in–cell scheme. *Physics of Plasmas*, 19:084501, 2012.

[72] A. Stern, Y. Tong, M. Desbrun, and J. E. Marsden. Geometric computational electrodynamics with variational integrators and discrete differential forms. In *Geometry, mechanics, and dynamics: the legacy of Jerry Marsden*, Fields Institute Communications. Springer, 2014. in press.

[73] T. Umeda, Y. Omura, T. Tominaga, and H. Matsumoto. A new charge conservation method in electromagnetic particle-in-cell simulations. *Computer Physics Communications*, 156(1):73–85, 2003.

[74] J. Villasenor and O. Buneman. Rigorous charge conservation for local electromagnetic field solvers. *Computer Physics Communications*, 69(2):306–316, 1992.

[75] Karl F. Warnick and Peter H. Russer. Two, Three and Four-Dimensional Electromagnetics Using Differential Forms. *Turkish Journal Of Electrical Engineering & Computer Sciences*, 14(1):153–172, 2006.

[76] Karl F. Warnick, Richard H. Selfridge, and David V. Arnold. Teaching Electromagnetic Field Theory Using Differential Forms. *IEEE Transactions on Education*, 1: 53–68, 1998.

[77] Erich S. Weibel. Spontaneously growing trensverse waves in a plasma due to an anisotropic velocity distribution. *Physical Review Letters*, 2:83–84, 1959.

[78] Alan Weinstein and Philip J. Morrison. Comments on: The Maxwell-Vlasov equations as a continuous hamiltonian system. *Physics Letters A*, 86(4):235–236, 1981. doi: 10.1016/0375-9601(81)90496-5.

[79] Jianyuan Xiao, Hong Qin, Jian Liu, Yang He, Ruili Zhang, and Yajuan Sun. Explicit high-order non-canonical symplectic particle-in-cell algorithms for Vlasov-Maxwell systems. *Physics of Plasmas*, 22:112504, 2015.

[80] Huanchun Ye and P. J. Morrison. Action principles for the vlasov equation. *Physics of Fluids B*, 4(4):771–777, 1992. doi: http://dx.doi.org/10.1063/1.860231. URL http://scitation.aip.org/content/aip/journal/pofb/4/4/10.1063/1.860231.

[81] K.S. Yee. Numerical solution of initial boundary value problems involving maxwell's equations in isotropic media. *IEEE Trans. Antennas Propag.*, 14:302–307, 1966.

[82] J. Yu, X. Jin, W. Zhou, B. Li, and Y. Gu. High-order interpolation algorithms for charge conservation in particle-in-cell simulations. *Commun. Comput. Phys*, 13: 1194–1150, 2013.